8-2014

Eastern US Dryline Climatology and Synoptic-Scale Environment

Rebecca S. Duell
University of Nebraska-Lincoln, rebecca.duell@huskers.unl.edu

EASTERN US DRYLINE CLIMATOLOGY AND SYNOPTIC-SCALE ENVIRONMENT

By

Rebecca Siân Duell

A THESIS

Presented to the Faculty of
The Graduate College at the University of Nebraska
In Partial Fulfillment of Requirements
For the Degree of Master of Science

Major: Earth and Atmospheric Sciences

Under the Supervision of Professor Matthew Van Den Broeke

Lincoln, Nebraska

July 2014

EASTERN US DRYLINE CLIMATOLOGY AND SYNOPTIC-SCALE ENVIRONMENT

Rebecca Duell, M.S.

University of Nebraska, 2014

Advisor: Matthew Van Den Broeke

The dryline is an important focal point for convection initiation, and the subject of many studies. While the most common location for drylines is the southern Great Plains, dryline passages and subsequent severe weather outbreaks have been documented in the Mississippi River Valley and into portions of the southeastern United States. Little is known about these "eastern" drylines or how often they occur, as no climatologies or detailed studies have been published on them. This thesis presents a fifteen-year climatology (1999-2013) of eastern drylines in an effort to identify how often and where they typically occur, and to identify synoptic patterns that result in drylines moving atypically far eastward. A computer algorithm was created that objectively identifies drylines from the North American Regional Reanalysis (NARR) dataset. Dryline events were divided into regional categories once the climatology of eastern drylines was compiled, and mean and anomaly synoptic composites were created of different variables for each regional category. Thirty-nine eastern drylines were identified through the study. These events occurred under synoptically-active conditions with amplified upper-air patterns, 500 mb shortwave troughs to the west or northwest of the drylines, and strong surface cyclones to the north.

Acknowledgements

I would like to express my deepest appreciation for those who have helped me complete this work. First and foremost, I would like to thank my advisor, Dr. Matthew Van Den Broeke, for all of his guidance and assistance in this research project as well as for his mentorship through graduate school. I would also like to thank my committee members, Dr. Mark Anderson and Dr. Adam Houston for their insight and guidance on this project. I'd also like to thank the meteorology faculty at the University of Nebraska–Lincoln, including my committee members and Dr. Clint Rowe and Dr. Jun Wang, whose graduate courses greatly increased my understanding of meteorology and my passion for the field. I would also like to thank the Department of Earth and Atmospheric Sciences at the University of Nebraska–Lincoln for the Research Assistantship that funded me throughout graduate school.

I would like to thank my family and friends back home for their continued support of my work, their trips to Nebraska to keep me motivated, and all of their words of encouragement. I would like to thank Nathan Huffman for all of his support and for patiently teaching me to program and to debug - skills that I would not have been able to complete this thesis without. Finally, but certainly not least, I would like to thank all of my fellow graduate students in the Department of Earth and Atmospheric Sciences. They have been my pseudo-family here in Nebraska and I wouldn't have been able to complete this work without their help, suggestions, and of course their humor.

Table of Contents

1. Introduction……..……..……1
2. Background…….……..…….3
I. Formation of the Dryline……..……..3
II. Quiescent vs. Synoptically-Active Drylines……..……..……4
III. Dryline Climatologies……..……..……4
IV. Synoptic Analyses……..……7
V. Project Motivation ……..……..……10
3. Methodology……...……..……..……...17
I. Dryline Identification……..……..……..17
II. Synoptic Composites……..……..20
4. Eastern Dryline Climatology……..……..…….23
5. NOAA HYSPLIT Model Backwards Parcel Trajectories….31
6. Regional Composites……...…….……34
a) Louisiana and Arkansas Drylines……..……..……34
b) Missouri, Iowa, and Illinois Drylines……..……..……..42
c) Alabama and Mississippi Drylines……..……..……50
7. Eastern Dryline Analysis…….……63
8. Conclusions……...……75

References…….……...77

LIST OF MULTIMEDIA OBJECTS

Fig. 2.1: Strong vs. weak dryline composites (From Schultz et al. 2007)……..…..9

Fig. 2.2: 1400 CST surface map for 18 March 1925 (From Maddox et al. 2013).....11

Fig. 2.3: Meteogram for Cairo, Illinois, 18 March 1925 (From Maddox et al. 2013 ……..…12

Fig. 2.4: Positions of low and boundaries 18 March 1925 (From Maddox et al. 2013)……..….12

Fig. 2.5: 0000 UTC surface analysis for 4 April 1974 (From Hoxit and Chappell 1975)…..…..13

Fig. 2.6: Tracks of tornadoes during Super Outbreak (From Locatelli et al. 2002)…….14

Fig. 2.7: Surface analysis for 0000 UTC 20 March 2003 ……..….15

Fig. 2.8: Surface Analysis for 1800 UTC 27 April 2011……..…16

Fig. 3.1: Study domain…….…….19

Table 3.1: Flagged grid point identification criteria……19

Table 3.2: Louisiana and Arkansas dryline dates…….……..……...…21

Table 3.3: Missouri, Iowa, and Illinois dryline dates…….…….....…….22

Table 3.4: Alabama and Mississippi dryline dates……..……22

Fig. 4.1: Number of dryline passages per point……...……24

Fig. 4.2: Number of dryline observed in each state……....…..25

Fig. 4.3: Number of eastern dryline passages per month…….……26

Fig. 4.4: Maximum observed dryline longitude and latitude by month……..27,28

Fig. 4.5: Maximum observed dryline longitude vs. cyclone strength…….….30

Fig. 5.1: NOAA HYSPLIT Model backwards parcel trajectories…….....33

Fig. 6.1: 250 mb vector wind composites for Louisiana and Arkansas drylines……..…….....36

Fig. 6.2: 500 mb geopotential height composites for Louisiana and Arkansas drylines…...…...37

Fig. 6.3: 850 mb zonal wind composites for Louisiana and Arkansas drylines……....38

Fig. 6.4: 850 mb meridional wind composites for Louisiana and Arkansas drylines……..….39

Fig 6.5: 850 mb temperature composites for Louisiana and Arkansas drylines…….....40

Fig 6.6: Sea-level pressure composites for Louisiana and Arkansas drylines……41

Fig. 6.7: 250 mb vector wind composites for Missouri, Iowa, and Illinois drylines……..44

Fig. 6.8: 500 mb geopotential height composites for Missouri, Iowa, and Illinois drylines…..45

Fig. 6.9: 850 mb zonal wind composites for Missouri, Iowa, and Illinois dryines…….....46

Fig. 6.10: 850 mb meridional wind composites for Missouri, Iowa, and Illinois drylines……...47

Fig. 6.11: 850 mb temperature composites for Missouri, Iowa, and Illinois drylines……....…48

Fig. 6.12: Sea-level pressure composites for Missouri, Iowa, and Illinois drylines……...49

Fig. 6.13: 250 mb vector wind composites for Alabama and Mississippi drylines……....53

Fig. 6.14: 500 mb geopotential height composites for Alabama and Mississippi drylines…....54

Fig. 6.15: 850 mb zonal wind composites for Alabama and Mississippi drylines…….…....55

Fig. 6.16: 850 mb meridional wind composites for Alabama and Mississippi drylines….……56

Fig. 6.17: 850 mb temperature composites for Alabama and Mississippi drylines……....….57

Fig. 6.13: Sea-level pressure composites for Alabama and Mississippi drylines……..…..58

Fig. 7.1: Surface analysis for 0300 UTC 25 February 2007……...….66

Fig. 7.2: Backwards parcel trajectories for 0300 UTC 25 February 2007……..…….67

Fig. 7.3: Surface map for 0300 UTC 25 February 2007…….……68

Fig. 7.4: Surface analysis for 1800 UTC 11 February 2009 ……..…..69

Fig. 7.5: Backwards parcel trajectories for 1800 UTC 11 February 2009 ……..….70

Fig. 7.6: Surface map for 1800 UTC 11 February 2009 ……71

Fig. 7.7: Surface analysis for 1800 UTC 2 April 2010 ……..…….……..…..72

Fig. 7.8: Backwards parcel trajectories for 1800 UTC 2 April 2010 ……..……...….73

Fig. 7.8: Surface map for 1800 UTC 2 April 2010 ……..……..…….74

1. Introduction

The dryline is an airmass boundary that marks a strong moisture gradient between a moist airmass and a dry airmass. In the United States, the dryline typically sets up meridionally over the Plains during spring and marks the gradient between the hot, dry air from the Mexican Plateau and the warm, moist air originating over the Gulf of Mexico. The dryline is also a zone of enhanced convergence, which makes it a focal point for convection initiation (e.g. Rhea 1966, Schaefer 1974, Schaefer 1986, Hane et al. 1997, Atkins et al. 1998, Hoch and Markowski 2005, Weiss et al. 2006, Schultz et al. 2007). A number of climatologies have been published (e.g., Rhea 1966, Schaefer 1974, Hoch and Markowski 2005), but they have all focused on Great Plains drylines. Hoch and Markowski (2005) found that the distribution in dryline longitudes at 0000 UTC peaks at near 101°W and that drylines become rare east of 95°W. However, little is known about these drylines that move atypically far eastward due to a lack of climatology of these boundaries. The focus of this project is to study drylines that move east of 95°W and to examine the synoptic setup associated with such events.

This research project has two primary objectives:

I) Create a fifteen year climatology of dryline passages east of 95°W.

II) Construct composites of synoptic conditions associated with eastern drylines.

This climatology is the first (to the author's knowledge) to document the frequency and importance of dryline passages in the eastern portion of the United States. The composites will enable identification of synoptic patterns resulting in continental tropical (cT) air being advected atypically far eastward, which will ideally aid forecasters

in more accurately forecasting future eastern dryline events.

2. Background

I. Formation of the Dryline

A background zonal water vapor gradient exists across the southern Plains due to differential moisture advection, where warm, moist maritime tropical (mT) air from the Gulf of Mexico is advected over the eastern Plains and hot, dry (cT) air from the Mexican Plateau is advected over the western Plains (Lin 2010). This differential moisture advection results in a large-scale background water vapor gradient generally located over the southern Plains. The background water vapor gradient is amplified through differential mixing between the deep cT airmass and the shallow mT airmass (Lin 2010) and differential evapotranspiration due to a strong east to west soil moisture gradient across the Plains, (Schaefer 1974, Schaefer 1986, Benjamin and Carlson 1986, Sun and Wu 1992, Peckham and Wicker 2000).

In order for the dryline to be established, the existing background water vapor gradient needs to be strengthened to form the very sharp moisture gradient that defines the dryline. One mechanism that accomplishes this is lee troughing. Troughs that form in the lee of the Rocky Mountains lead to geostrophic deformation of the wind field, which, through stretching and confluence of the moisture gradient, can result in the creation of a dryline. Lee troughing also enhances the southeasterly flow off the Gulf of Mexico, increasing convergence along the dryline (Benjamin and Carlson 1986) and sharpening the moisture gradient by bringing deeper mT air farther west. In addition to lee troughing, mesoscale frontogenesis along the dryline enhances the moisture gradient (Ziegler et al. 1995, Schultz et al. 2007).

II. Quiescent vs. Synoptically-Active Drylines

It has been suggested that drylines can be divided into quiescent and synoptically-active categories (Schaeffer 1986, Hane et al. 2002, Hane et al. 2004). Quiescent drylines occur under quiet synoptic conditions. The motion of quiescent drylines is primarily controlled by vertical mixing, which results in the typical eastward movement during the day, with westward retrogression after sunset (e.g. Schaefer 1986). Synoptically-active drylines occur under synoptically-active conditions – that is, they often extend equatorward from intense low pressure systems (Hane et al. 2002), are located downstream from shortwave troughs, and tend to be associated with highly-amplified upper-air patterns. The motion of synoptically-active drylines is primarily controlled by synoptic-scale processes, which dominate the small-scale vertical mixing that controls the motion of quiescent drylines (Schultz et al. 2007). In synoptically-active dryline cases, synoptic forcing is responsible for advecting the arid air aloft from the Mexican Plateau eastward. Vertical mixing then transports the dry air from aloft down to the surface west of the dryline. Synoptic scale forcing can transport the cT airmass farther eastward than vertical mixing alone; thus, synoptically-active drylines often move much farther east than quiescent drylines. It is therefore hypothesized that active synoptic conditions will be necessary for the occurrence of drylines east of 96°W.

III. Dryline Climatologies

The few climatologies of drylines published in the literature have focused on Great Plains drylines in the spring months. The first published climatology of the dryline was created in 1966 by Rhea and spanned the months of April, May, and June of 1959-

1962. Three-hourly surface charts were used for determining the dryline position. Hourly radar summaries were examined to find thunderstorm development along identified drylines. Rhea defined drylines as an "organized dew-point discontinuity zone of at least 10°F existing between one or more reporting points and the nearest neighboring reporting point" (Rhea 1966, p. 59). Using this definition, Rhea identified drylines on 45% of days included within the study. The study domain was not mentioned in the paper, nor was any information about the location of the observed drylines.

Schaeffer (1974) published a climatology of drylines with additional criteria for dryline identification. His climatology consisted of three years (1966 – 1968), and, like Rhea, Schaeffer's climatology focused on the spring months (April, May and June). Schaeffer's climatology was based on four criteria used to identify drylines:

1) A dewpoint difference of at least 10°F was required between reporting stations, with the additional requirement that the gradient had to exist between several pairs of stations and had to last at least six hours.

2) Dewpoints in the moist airmass were required to have a mean value of at least 15°C (50 °F).

3) The dryline had to exist in the afternoon and the virtual temperature gradient needed to be small.

4) A diurnal change in the direction of the temperature gradient was required.

Schaeffer identified drylines on 41% of his study days, similar to Rhea's (1966) findings. The domain of Schaeffer's study was also not mentioned, however it was mentioned that drylines that move east of 96°W become too diffuse to be recognizable (Schaeffer 1974), suggesting that his climatology consisted only of drylines west of

96°W.

Hoch and Markowski (2005) created a 30-year (1973-2002) dryline climatology for the Great Plains for the months of April, May, and June which showed results for the domain 105°W to 93°W. Like Rhea (1966) and Schaeffer (1974), surface data was used by Hoch and Markowski to identify drylines. Hoch and Markowski's surface data came from Automated Surface Observing System (ASOS) stations and only included 0000 UTC data. Their qualitative definition of drylines was "confluent boundaries separating a dry, continental, tropical airmass from a much more humid airmass" (Hoch and Markowski 2005, p. 2133). The criterion used to identify drylines in their study was a specific humidity gradient of at least 3 x 10^{-8} m^{-1} (3 g kg^{-1} per 100 km). Thirty two percent of days included in their study had a 0000 UTC dryline present in the Great Plains, with a broad peak in mid to late May. They found a well-defined peak in 0000 UTC dryline position near 101°W longitude and also observed that the climatological dryline position drifts westward through the spring.

Schultz et al. (2007) constructed a dataset of drylines that occurred in western Texas during April, May, and June of 2004 and 2005 using surface data from the West Texas Mesonet. They used this dataset to study the synoptic regulation of dryline intensity, and selected drylines that met a number of criteria. A dewpoint gradient had to be present and had to have an eastward (down-terrain) component with the majority of the gradient residing in the West Texas Mesonet domain. The gradient could not be attributed to a cold front or warm front and could not be influenced by convective outflow. The gradient needed to increase between 0700 and 1800 local time (LT). Finally, the region of maximum dewpoint gradient was required to either slow down its

eastward progress or move westward after 1800 LT. Using these criteria, they found drylines to be present on 35% of study days (Schultz et al. 2007).

IV. Synoptic Analyses

Recently, there has been a surge of field projects that have allowed for detailed mesoscale observational analysis of drylines. These projects include Verifications of the Origins of Rotation in Tornadoes Experiment (VORTEX; Rasmussen et al. 1994), Central Oklahoma Profiler Studies project (COPS-91), and the International H_2O Project (IHOP; Weckwerth et al. 2004), among others. Much has been learned about the mesoscale processes that control dryline strength and movement from these studies. However, there has been less focus on the larger- (synoptic-) scale processes that contribute to dryline strength and movement.

Though Hoch and Markowski's (2005) study of drylines primarily focused on Great Plains drylines, they did remark that "virtually all dryline passages east of roughly 97°W longitude are associated with migrating cyclones" (Hoch and Markowski 2005, p. 2134-2135). Examination of atmospheric soundings on dryline days showed a positive correlation between westerly momentum in the lower to middle troposphere and dryline longitude. Hoch and Markowski also noted drylines are observed increasingly farther west as the spring progresses, which they suggested was most likely due to the retreat of the polar jet stream to the north throughout the spring, causing a decrease in the westerly component aloft in the region as spring progresses.

Schultz et al. (2007) investigated the role of synoptic-scale processes in regulating the strength of the dryline. Their two-year, springtime climatology of dryline days

identified a total of 64 cases. All of the cases were ranked according to *dryline intensity* (ΔT_d). Cases in the top quartile were termed strong dryline days, and cases in the bottom quartile were termed weak dryline days. Synoptic composites were created for strong and weak drylines, which identified synoptic-scale patterns that regulate dryline intensity. The results (Fig. 2.1) showed that the strongest drylines in western Texas had a 250 mb jet maximum of 25-30 m s^{-1} over the eastern Pacific Ocean, a 500 mb slightly negative-tilted short-wave trough over the western United States approaching Texas, and a surface cyclone over eastern New Mexico and western Texas. In contrast, weak drylines had a 250 mb jet located much farther poleward over the north central United States and central Canada, a 500 mb ridge over the central United States, and a much broader area of low pressure over the southwestern United States and northwestern Mexico.

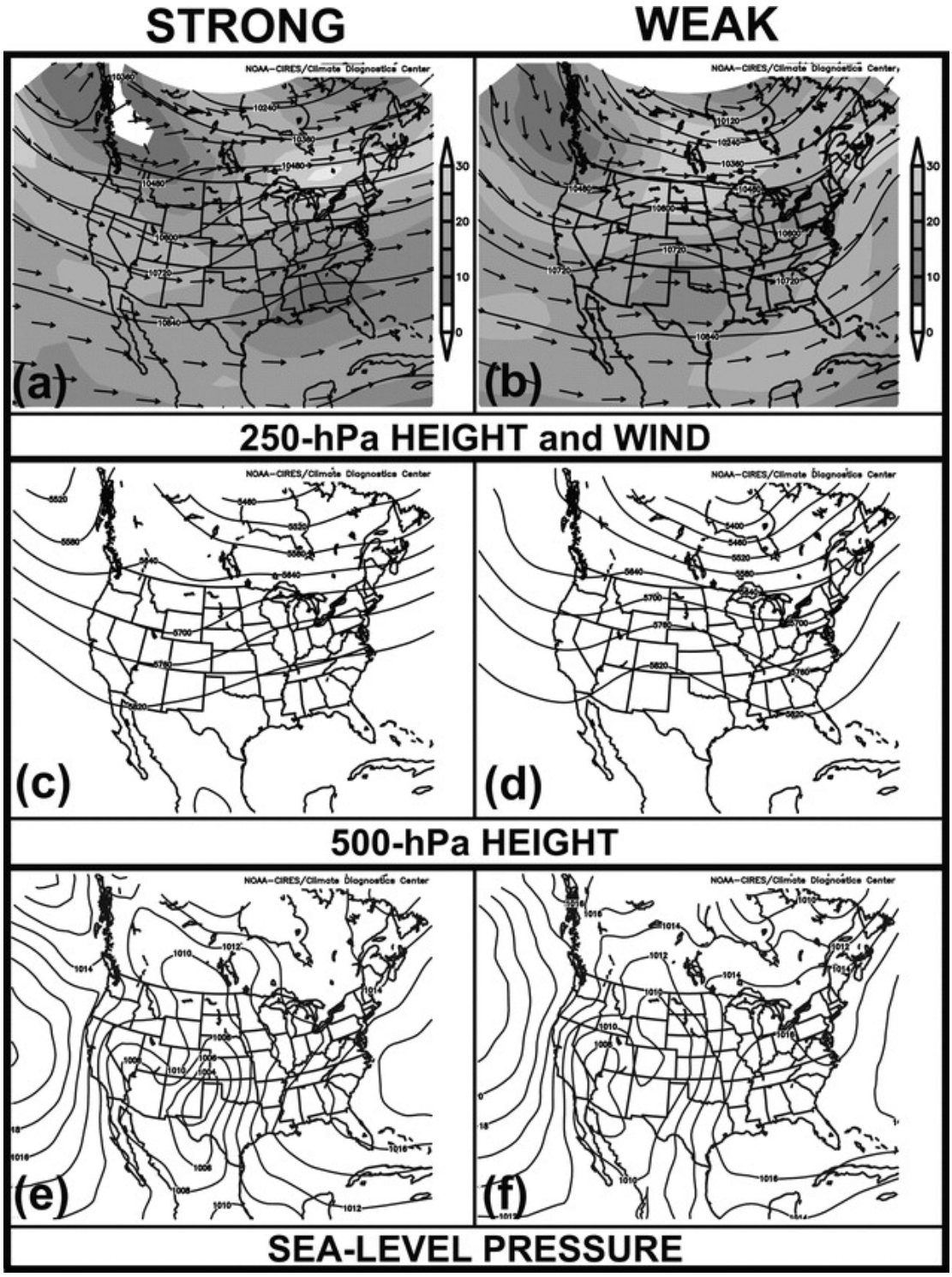

Figure 2.1: Strong (left) vs. Weak (right) dryline composites: (a) and (b) 250 mb geopotential height; solid lines; contour interval 120 m, wind speed (m s^{-1}), shaded according to scale, and wind direction (vectors); (c) and (d) 500 mb geopotential height, solid lines; contour interval 60 m; (e) and (f) sea level pressure solid lines; contour interval 2 mb. (Figure 3 from Schultz et al. 2007.)

V. Project Motivation

The vast majority of research on drylines has focused on drylines in the Great Plains region. While the Great Plains is the preferred location for drylines, forecasting experience shows that occasionally drylines will move farther east than 96˚W. However, due to the lack of a dryline climatology east of the Great Plains, it is unknown how often the dryline moves farther east. Additionally, most dryline studies have largely focused on quiescent drylines (e.g. Sun and Wu 1992, Peckham and Wicker 2000, Ziegler and Rasmussen 1998, Jones and Bannon 2002, Hane et al. 1997), the movement of which is dictated by subsynoptic-scale processes. While Schultz et al. (2007) addressed synoptic conditions that contribute to dryline intensity, the literature is relatively quiet on synoptic processes that result in drylines moving atypically far eastward.

Some of the deadliest tornado outbreaks east of the Great Plains have occurred on days when the dryline moved east of 96°W. On March 18, 1925, a severe weather outbreak across the Mississippi River Valley included a deadly tornado that tracked from southeastern Missouri through Illinois and into Indiana. This tornado, known as the "Tri-state tornado," had a death toll of approximately 695 people and remains the single deadliest tornado is United States history (Maddox et al. 2013). The newly analyzed surface analysis for the time of the Tri-state tornado is shown in Fig. 2.2. Figure 2.3 shows the meteogram for Cairo, Illinois (location in southern Illinois, shown as red star in Fig. 2.2), which clearly shows the dryline passage at 1500 CST, shortly before the passage of the cold front. The dryline moved all the way into southern Illinois in this event, allowing for the triple point (the intersection of the cold front, warm front, and the dryline) to progress into southeastern Missouri. The triple point is a favored position for

tornadic storms to develop, and was ultimately where the Tri-state tornado developed on this day (Moller 2011, Maddox et al. 2013). Figure 2.4 shows the time progression of the location of the synoptic boundaries on 18 March 1925, with the location of the tornado marked by colored triangles. In the case of the Tri-state tornado, an inversion aloft in the warm sector (a characteristic typical of warm sectors ahead of drylines) suppressed deep convective initiation until about 1500 CST, allowing for the supercell that contained the deadly Tri-state tornado to remain very isolated and largely uninfluenced by interactions with other storms for over 300 km.

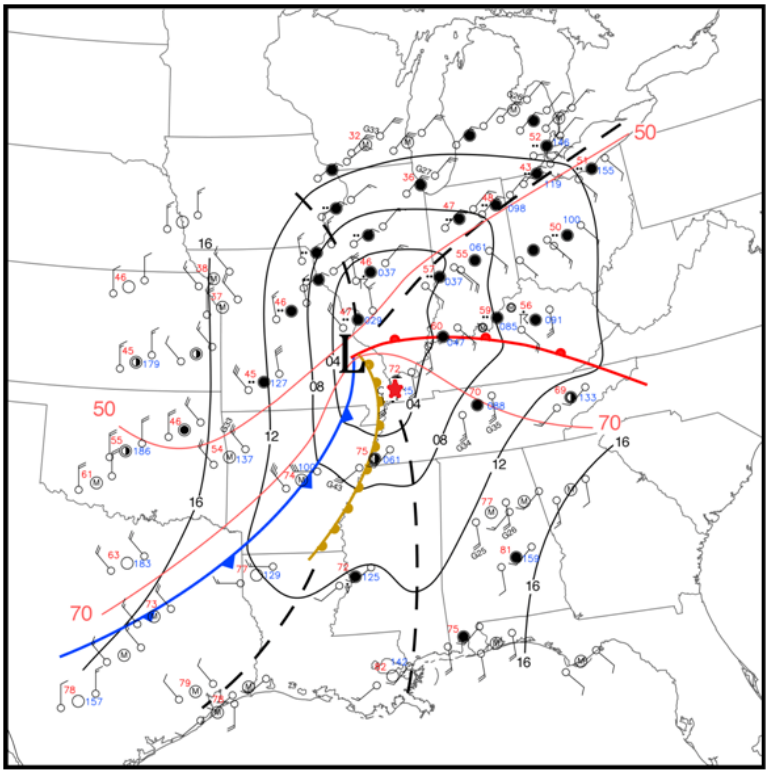

Figure 2.2: Newly-analyzed 1400 CST surface map for 18 March 1925. Fronts and dryline are indicated by standard symbols, along with pressure troughs (dashed) and mesoscale outflow boundary (dash with double dots). Pressures and isobars are in mb winds are in mph, and temperatures are in °F. Isotherms at 20°F intervals are red. Red star denotes location of Cairo, Illinois, the location of the meteogram from Figure 2.3 (Figure 8 from Maddox et al. 2013).

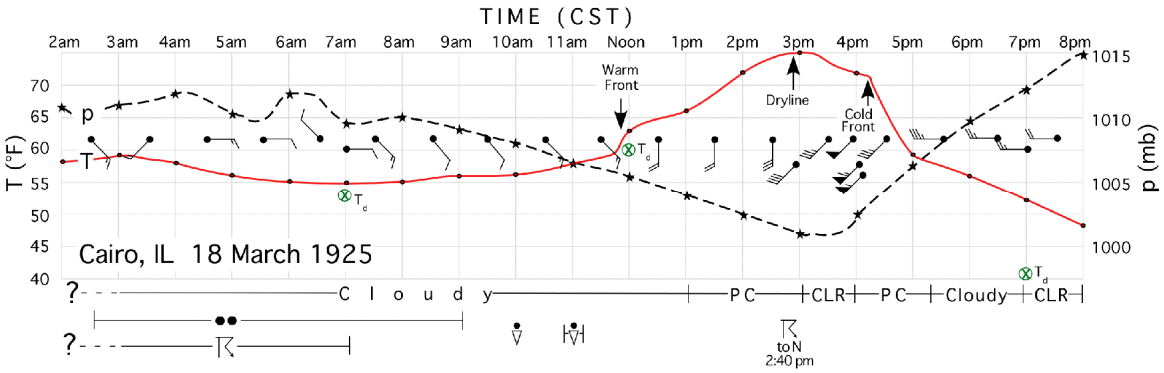

Figure 2.3: Meteogram for Cairo, Illinois, 18 March 1925. Pressures are in hPa; temperatures are in °F' dewpoints shows by small circles with "X"; winds are in mph, and time is CST. Clouds and weather conditions also are shown. Data are from WB forms 1001 and 1014, as well as from the original barograph and thermograph traces. (Figure 15 from Maddox et al. 2013).

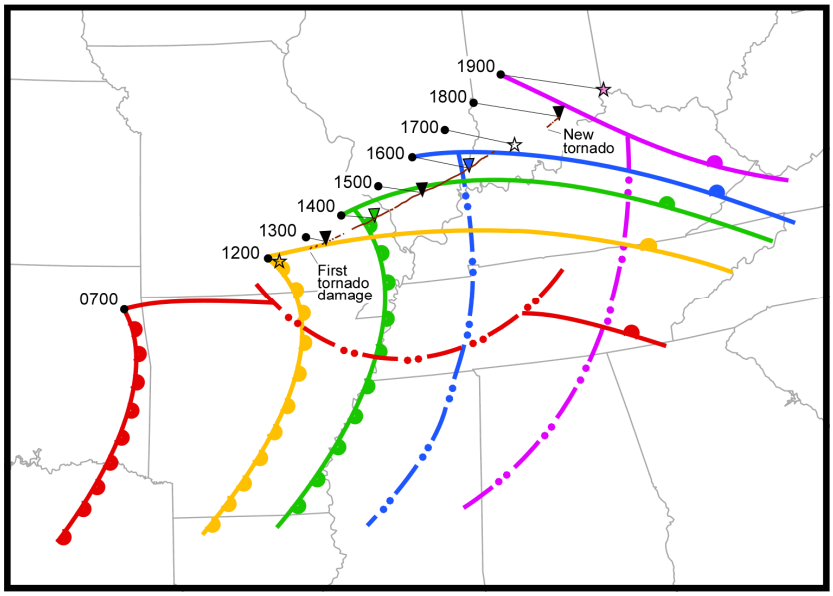

Figure 2.4: Positions of the synoptic low (black dots: 0700, 1200–1900 CST) and boundaries adjacent to the warm sector (dryline, warm front, and convective outflow boundaries) are shown. The Tri-State tornado (colored triangles) and extrapolated supercell positions (stars; 1200, 1700 and 1900 CST) are indicated. The tornado track, traced from the data points in Johns et al. (2013), is in dark brown. A thin black line connects the synoptic low pressure center and the tornado (or extrapolated supercell) position at each time. Supercell positions at 1200, 1700, and 1900 CST were estimated using the average speed of the tornado. Only a portion of the outflow boundary is shown for 0700 CST. (Figure 12 from Maddox et al. 2013).

The “Super Outbreak” of 1974 was another deadly tornado outbreak that occurred on a day when the dryline moved into the Mississippi River Valley (Fig. 2.5) On 3 April 1974, 148 tornadoes were spawned east of the Mississippi River along three different squall lines (Locatelli et al. 2002). Figure 2.6 shows the tracks of the tornadoes labeled by the squall line with which they were associated. Locatelli et al. found that the most violent tornadoes were associated with the second squall line, which was spawned when a cold front aloft occluded with the dryline (Locatelli et al. 2002).

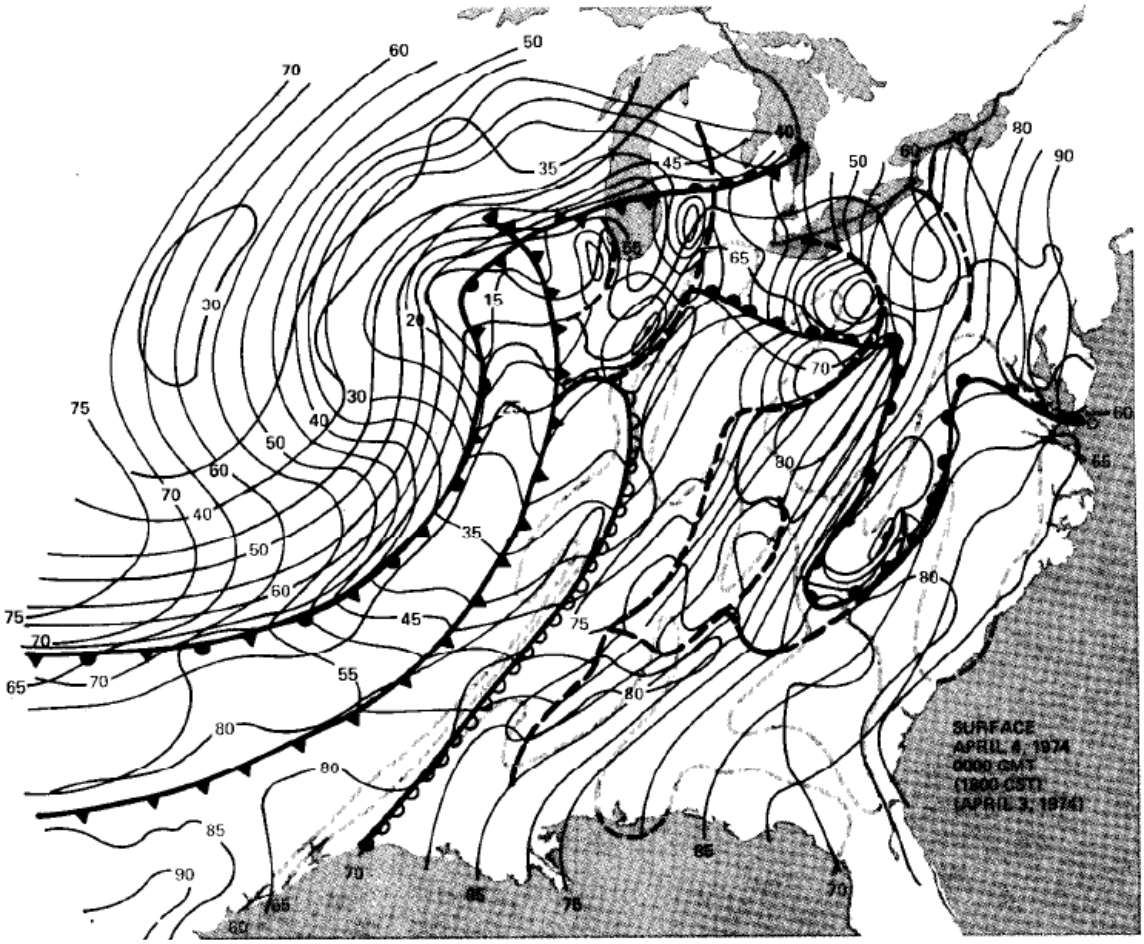

Figure 2.5: Surface analysis at 0000 UTC 4 April 1974. Isotherms (black), 5°F intervals; isodrosotherms (gray), 5°F intervals for values ≥ 60°F; squall lines, mesoscale troughs, and outflow boundaries, dashed lines. (Figure 26 from Hoxit and Chappell 1975).

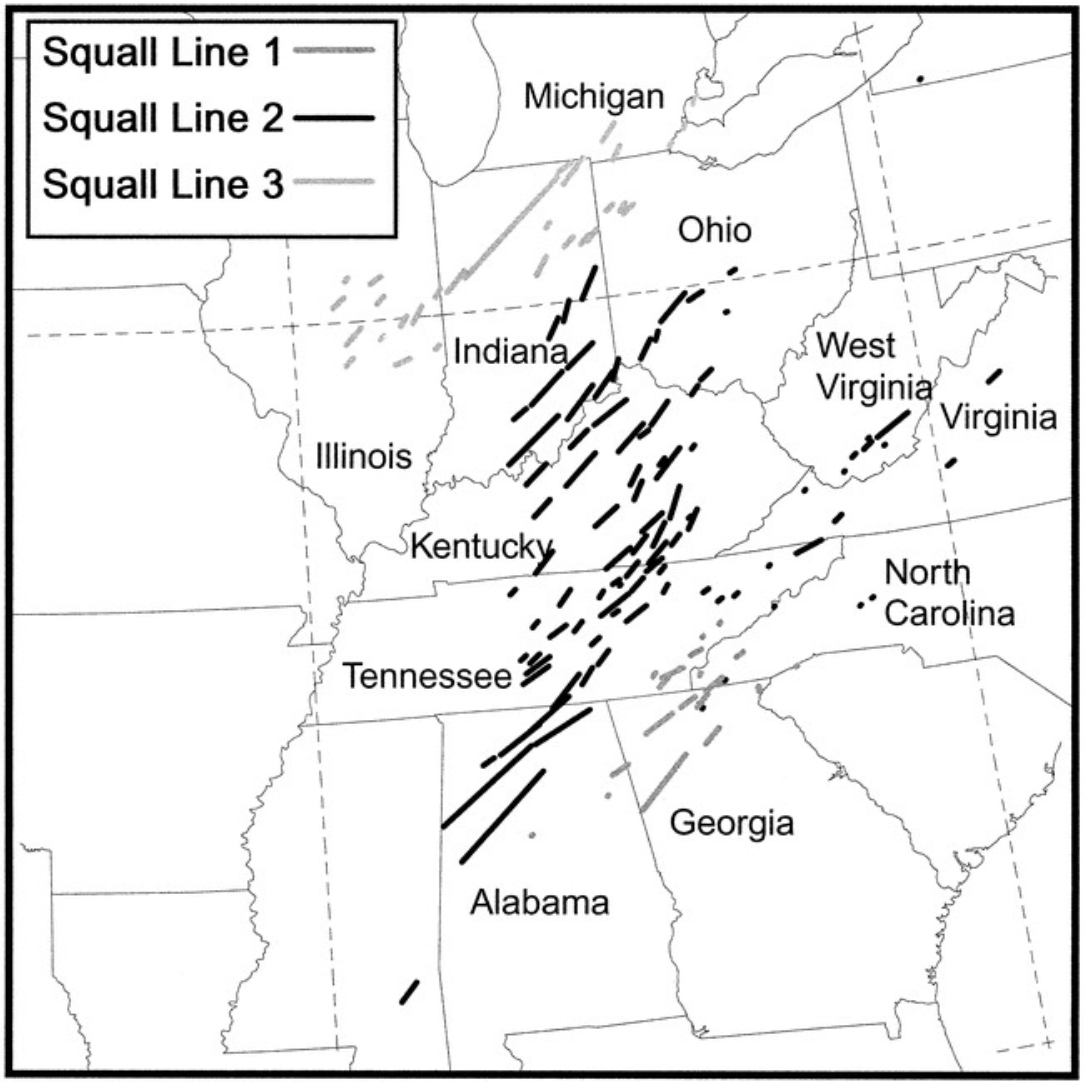

Figure 2.6: Tracks of tornadoes during the Super Outbreak of 2–5 April 1974. Tornado tracks are labeled by the squall line with which they were associated. Tornadoes associated with Squall Line 2 were closely related to a dryline. (Figure 3 from Locatelli et al. 2002).

Barbré et al. (2005) presented a poster on the dryline that occurred in Alabama on 19 March 2003. Their study used synoptic weather maps, soundings from 1200 UTC 19 March 2003 to 0000 UTC 21 March 2003, satellite imagery, Weather Surveillance Radar (WSR-88D) and instruments from the University of Alabama in Huntsville's Mobile Integrated Profiling System (MIPS) to perform an in-depth analysis of the dryline event.

Despite a highly-sheared environment and little Convective Available Potential Energy (CAPE), moisture convergence associated with the dryline was able to initiate storms which spawned 22 tornadoes in the region. This was a very rare event to have a dryline move all the way into Alabama, and is an example of how far east a dryline is able to move and have a significant impact on severe weather outcome.

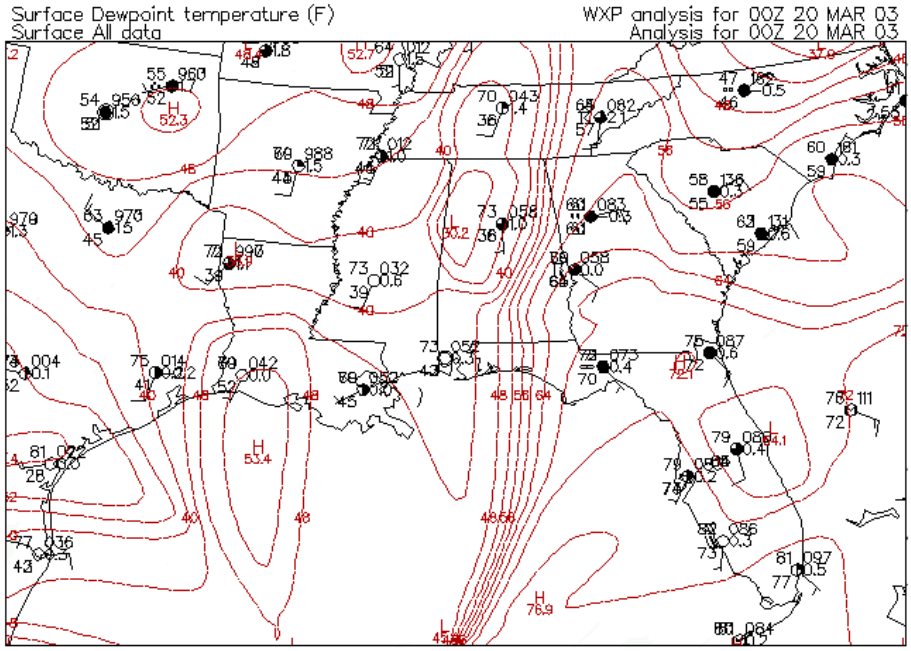

Figure 2.7: Surface analysis from 0000 UTC 20 March 2003 showing station plots and 4°F isodrosotherms in red. Note the dryline in eastern Alabama. Plot courtesy of Plymouth State Weather Center.

One of the most significant tornado outbreaks in recent history, which occurred on 27 April 2011, resulted in 199 confirmed tornadoes and 319 fatalities (Knupp et al. 2013), also occurred on a day when the dryline progressed farther east than usual. Figure 2.8 shows the 1800 UTC surface analysis on 27 April 2011 by the Hydrometeorological Prediction Center (HPC, 2013). The dryline extended southward from a low pressure system through Arkansas and Louisiana, around the location where the first supercells of

the outbreak were initiated.

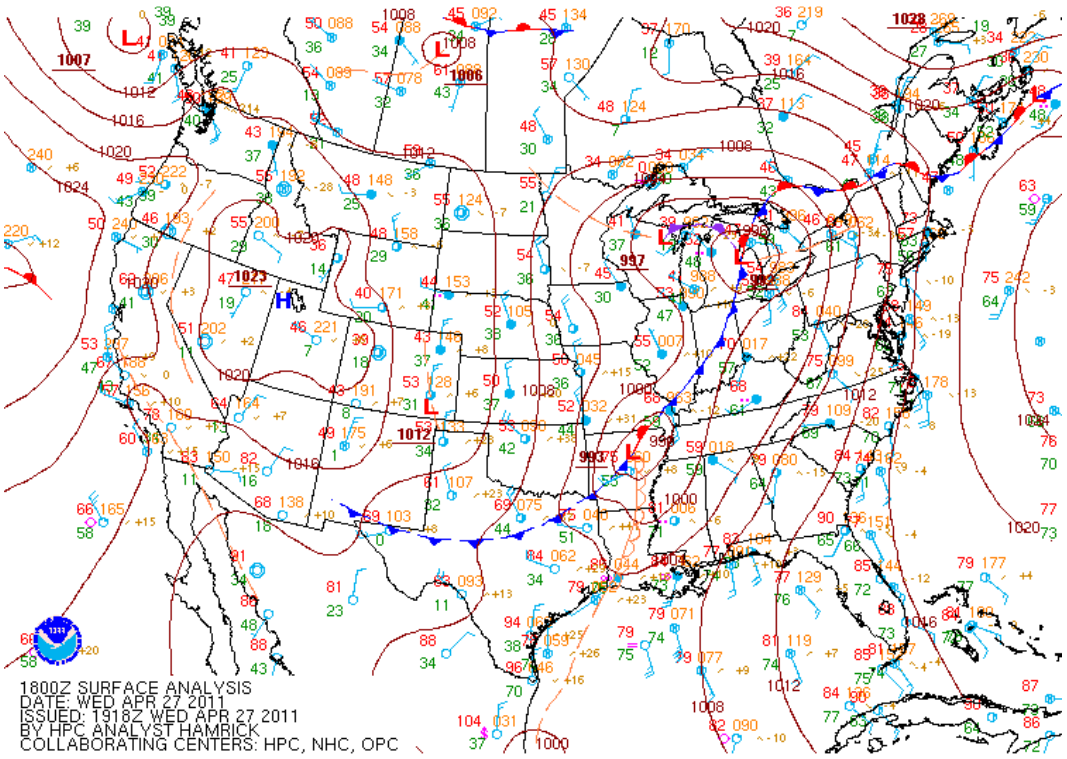

Figure 2.8: Hydrometeorological Prediction Center (HPC) surface analysis from 1800 UTC 27 April 2011. From the HPC surface analysis archives.

While different studies have shown that significant severe weather outbreaks have occurred on days when drylines move east of 96°W, little is known climatologically about these drylines or the severe weather associated with them. A climatology of eastern drylines will give us an idea of how often they occur. The synoptic composites created will enable identification of synoptic patterns resulting in drylines moving atypically eastward. Once these patterns are established, forecasters will be able to more accurately forecast future eastern dryline passages based on the synoptic conditions, ideally allowing for more accurate advanced warnings of potentially significant severe weather outbreaks associated with eastern dryline pass

3. Methodology

I. Dryline Identification

A computer algorithm was written that identified points that fall along drylines in the study's domain (Fig. 3.1) according to three criteria (see Table 3.1 for a bulleted list of the criteria). The domain of the study included the entire states of Louisiana, Arkansas, Missouri, Iowa, Illinois, Indiana, Mississippi, and Alabama, and parts of the states of Kentucky and Tennessee along with a portion of the Florida Panhandle. Being consistent with the approach of Hoch and Markowski (2005), a specific humidity gradient of at least 3×10^{-8} m^{-1} (3 g kg^{-1} per 100 km) is the first requirement to identify drylines. At this point, it becomes necessary to add additional criteria to attempt to separate drylines from frontal boundaries. The first criterion is modified such that the specific humidity value is required to be higher to the east than the west of the identified boundary. The second criterion used is a wind shift over 100 km across the boundary, characteristic of the dryline. The winds to the west of the boundary are required to be from between 170˚ and 280˚. The winds to the east of the boundary are required to be from between 80˚ and 190˚w. This wind shift from westerly or southwesterly to southerly or southeasterly is typical of the wind shift across the dryline, where the winds from the east originate over the Gulf of Mexico and the winds from the west originate from the Mexican Plateau. The final criterion used in this study is that the temperature gradient is required to be less than positive 0.02˚C km^{-1} from west to east. Since the dryline is an airmass boundary between two tropical airmasses (cT and mT) the temperature gradient across the boundary should be fairly small in comparison with a cold front. The wind shift criteria and the maximum temperature gradient criteria eliminate obvious cold fronts in which the winds had any

significantly northerly component, or there is a large temperature gradient across the boundary.

The computer algorithm used data from the National Centers for Environmental Prediction (NCEP) North American Regional Reanalysis (NARR) dataset (Earth System Research Laboratory, 2013). This is a high-resolution (32 km grid spacing) three-hourly atmospheric and land surface hydrology dataset for the North American domain (Mesinger et al. 2006). The NARR dataset was introduced in the mid 2000s and was developed as a major improvement to earlier datasets due to its resolution and its accuracy through the use of additional sources of data, improved data processing, and several Eta model developments (Mesinger et al. 2006). While not used yet to specifically identify drylines in the published literature, computer algorithms ingesting NARR data have been used in other studies to identify mesoscale features (e.g. identification of west coast thermal troughs [Brewer et al. 2012] and identification of strong intermountain cold fronts [Shafer and Steenburgh 2008]).

Each grid point in the domain was run through the algorithm and flagged if it met all three criteria. Flagged points are then run through an additional criterion that required two or more adjacent flagged points in order to rule out small scale boundaries or other discontinuities. Flagged points are then organized into a list of dryline days, which are manually quality controlled to ensure any remaining obvious fronts, sea-breeze boundaries, and outflow boundaries are excluded from the dryline dataset. Finally, air parcels on either side of the remaining flagged identified drylines are run through NOAA's Hybrid Single-Particle Langrangian Integrated Trajectory (HYSPLIT) model to verify the origins of air parcels and to infer the position of the airmasses relative to the

boundaries. If parcels on the western side of the boundary are shown to originate off the Mexican Plateau and parcels on the east side of the boundary are shown to originate from over the Gulf of Mexico, then the boundary met all this study's requirements for the dryline and is added to the dryline database.

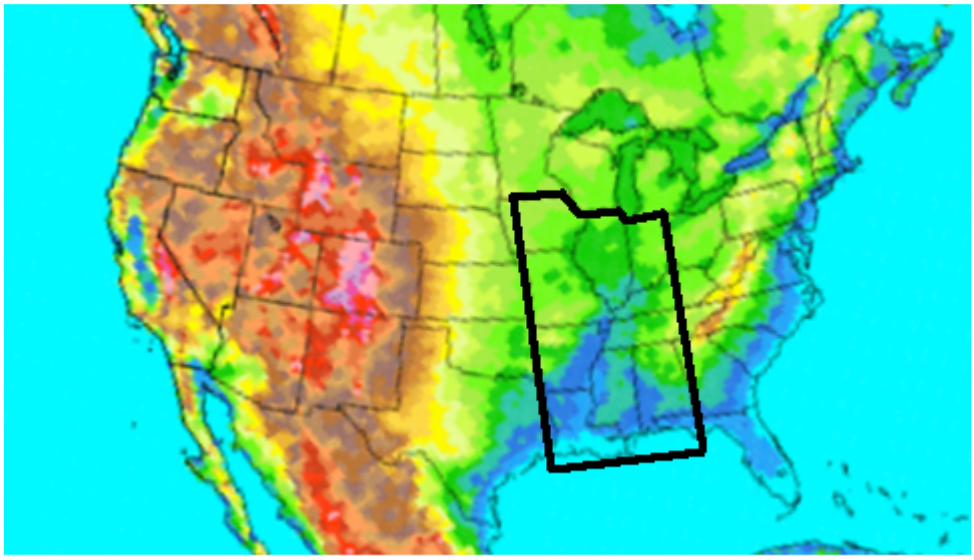

Figure 3.1: Study domain outlined in black on a topographical map. Figure adapted from Mesinger et al. 2006.

Table 3.1: Bulleted list of criteria used in computer algorithm to flag individual grid points

Flagged Grid Point Identification Criteria
• A specific humidity gradient of at least 3 x 10^{-8} m^{-1} (3 g kg^{-1} (100 $km)^{-1}$)
• Wind direction on the western side of the boundary from between 170˚ and 280˚. Wind direction on the eastern side of the boundary from between 80˚ and 190˚
• Temperature gradient across the boundary of < 0.02˚C km^{-1}

II. Synoptic Composites

Once the database of eastern drylines is created, synoptic features associated with the drylines are analyzed. Drylines are broken into three regional categories in an effort to identify synoptic features present at the time of and leading up to drylines in different regions. The regional categories are:

1) Louisiana and Arkansas drylines (25 days)

2) Missouri, Iowa, and Illinois drylines (16 days)

3) Mississippi and Alabama drylines (3 days)

Drylines used to create the Louisiana and Arkansas region are listed in Table 3.2, the Missouri, Iowa, and Illinois drylines are listed in Table 3.3, and the Mississippi and Alabama drylines are listed in Table 3.4. Three drylines overlapped and were included in the Louisiana and Arkansas regional composites as well as the Missouri, Iowa, and Illinois regional composites. Twenty-two of the 25 cases (88%) used in the Louisiana and Arkansas regional composites are unique to the first region, 13 of the 16 cases (81%) used in the Missouri, Iowa, and Illinois regional composites are unique to the second region, and 3 of the 3 cases (100%) used in the Mississippi and Alabama regional composites are unique to the third region. Composite fields and images are created for each of the regions at the National Oceanic and Atmospheric Administration (NOAA) / Earth System Research Laboratory (ESRL) Physical Sciences Division, Boulder, Colorado, from their website at http://www.esrl.noaa.gov/psd/. The NCEP/NCAR Reanalysis dataset, a research-quality dataset with data dating back to 1948 (Kalnay et al. 1996), was used to create the composites. The variables analyzed are: 250 mb vector winds, 500 mb geopotential heights, 850 mb zonal winds, 850 mb meridional winds, 850

mb temperatures, and sea-level pressure. For each variable, mean composites and anomaly composites are created and analyzed for dryline days in each region, with separate composites created for 24 hours before the event, 12 hours before the event, and the time of the event. The time of the event is chosen as the time at which the dryline progressed farthest east. The anomalies were compared to the 30 year (1981 through 2010) long-term mean.

Table 3.2: Dates that drylines were analyzed in Louisiana and/or Arkansas

Louisiana and Arkansas Dryline Dates
7 February 1999
10 April 1999
5 May 1999
3 January 2000
13 February 2000
24 April 2003
18 November 2003
5 March 2004
18 October 2004
21 February 2005
9 March 2006
7 April 2006
16 April 2006
2 April 2009
10 March 2010
27 April 2011
23 February 2012
16 December 2012
20 December 2012
10 February 2013

Table 3.3: Dates that drylines were analyzed in Missouri, Iowa and/or Illinois

Missouri, Iowa, and Illinois Dryline Dates
8 April 1999
8 March 2000
18 May 2000
7 April 2001
11 April 2001
4 May 2003
18 October 2004
7 April 2006
7 June 2007
2 April 2010
17 February 2011
10 April 2011
10 May 2011
22 February 2012
15 April 2012
10 February 2013

Table 3.4: Dates that drylines were analyzed in Alabama and/or Mississippi

Alabama and Mississippi Dryline Dates
19 March 2003
11 February 2009
24 January 2010

4. Eastern Dryline Climatology

A total of 39 eastern drylines were identified between 1999 and 2013. A map with the number of different dryline passages per point identified by the computer algorithm after quality control is presented in Fig. 4.1, with the approximate study domain outlined in black. Multiple hits on a single point for the same dryline have been removed in order to remove the bias of extra hits associated with slow moving drylines. The highest number of dryline passages per point (13) was observed in northwestern Louisiana, with the largest number of passages generally concentrated around northwestern Louisiana and southwestern Arkansas. Although northwestern Louisiana saw the most dryline passages, there were no dryline passages analyzed in southeastern Louisiana. Points in western Arkansas saw up to 10 passages, while points in western Iowa and western Missouri saw up to 6 passages. It makes sense that the western points of the domain generally saw more dryline passages than the eastern points, due to their closer proximity to the source of the cT air. Up to 2 drylines passages were observed in a single point in both Illinois and Mississippi.

The drylines that moved into Alabama and Mississippi did not appear to continuously move eastward, but rather appeared to move in a more stepwise fashion. This is likely an indication that the cT air in these cases was not advected eastward at low levels, but rather likely descended down from the Elevated Mixed Layer (EML) aloft. The stepwise movement of a drylines could also be attributed to a limitation of the dataset used in the study – the highest temporal resolution for the NARR dataset is three-hourly. When drylines moved rapidly eastward, points at which the dryline passed over between datasets were not able to be flagged. This likely resulted in an apparent stepwise

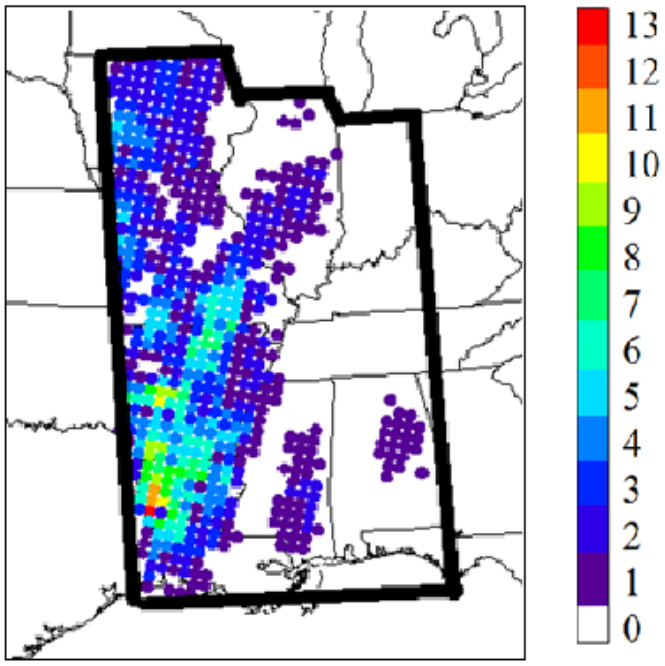

Figure 4.1: Number of dryline passages identified by the computer algorithm per point after quality control. Approximate study domain is outlined in black.

movement of the dryline in a number of cases that might not have been entirely accurate of the situation, and would have been mitigated by the use of a higher temporal resolution dataset.

Of the number of dryline passages through each state (Fig. 4.2), Arkansas had the most passages (19 passages), followed closely by Louisiana (15 passages) and Missouri (12 passages). This climatology shows that, while dryline passages east of the Great Plains states are uncommon, they do occur with sufficient frequency to be important in a climatological sense. Drylines move into Louisiana, Arkansas, and Missouri approximately once per year, and farther east approximately once per decade.

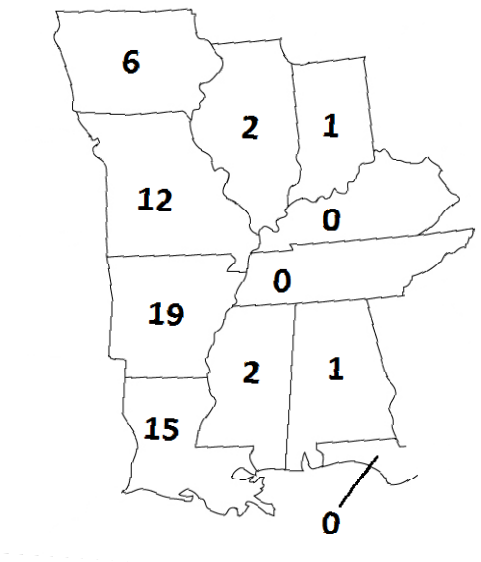

Figure 4.2: Number of drylines observed in each state from 1999 through 2013

Studies of Great Plains drylines have found late May and June to have the most dryline passages (Hoch and Markowski 2005, Schultz et al. 2007). However, eastern drylines peak earlier in the year, with the peak occurring between February and April (Fig. 4.3). This is likely due to the tendency for the polar jet and strong surface cyclones to be located farther south during these months – features generally required for these synoptically-active drylines to move into the Mississippi River Valley. The relationship between the synoptic features and the location of a dryline will be further explained later in this section and in section 5. No drylines are observed in the eastern domain between the months of July and September. The absence of drylines during these months can partially be attributed to the North American Monsoon (NAM), which acts to increase moisture over the Mexican Plateau during the late summer. A 30-year dewpoint climatology (Robinson 1998) shows an increase in dewpoints over the southwestern United States during the months of July, August, and September. During these months, any cT air that does get transported farther east will likely not be dry enough to establish

the specific humidity gradient of 3 x 10^{-8} m^{-1} (3 g kg^{-1} (100 km)$^{-1}$) that is required for this study, and thus will not result in a dryline. Another reason for the lack of eastern drylines during the late summer is likely the relative lack of strong westerly momentum aloft in the region.

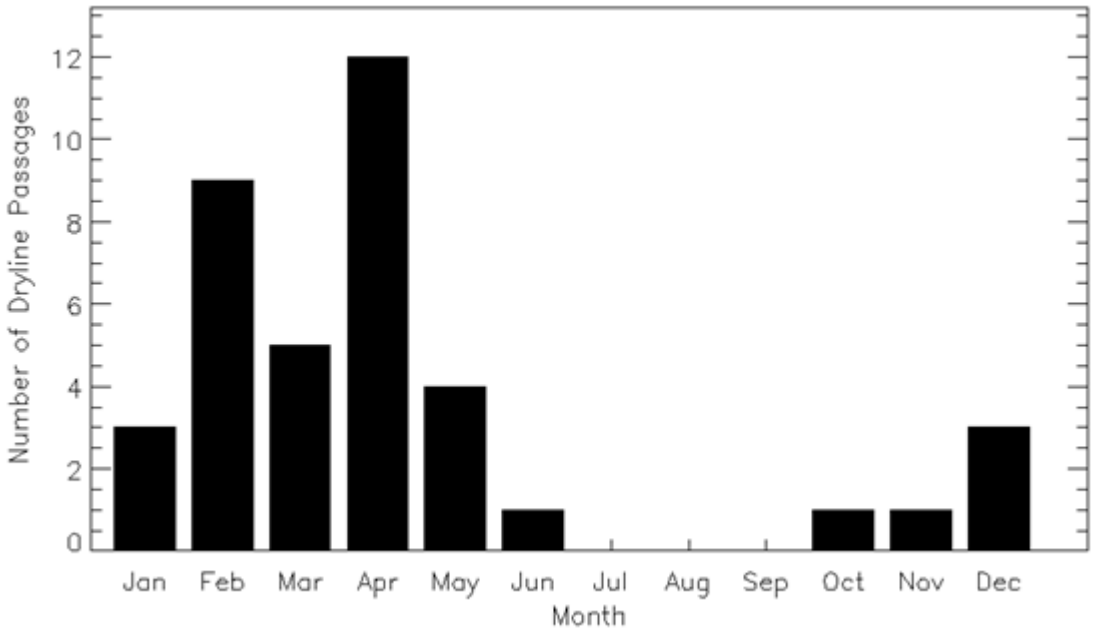

Figure 4.3: Number of dryline passages through domain per month

Figure 4.4a shows the farthest east longitude (in degrees West) that each dryline was analyzed at throughout the eastern dryline season (October through June). A linear line of best fit (not shown in Fig. 4.4a) has a coefficient of determination (R^2) value of .01, meaning that almost none of the variation in dryline longitude by time of year can be explained by a linear line of best fit (Wilks 2006). However, a parabolic line of best fit (shown in Fig. 4.4a) has a slightly better coefficient of determination value of approximately 0.06. While still a weak correlation, this does point to a more parabolic relationship between dryline longitude and time of year (i.e. drylines move farther east

during late winter and early spring, and not as far east during fall and late spring). There were no observed drylines that progressed east of 90°W outside of the months of January, February, and March (Fig. 4.4a). Figure 4.4b shows the maximum latitude (in degrees North) of each dryline throughout the eastern dryline season. The coefficient of determination value for this plot was 0.27. The plot shows an increase in dryline latitude throughout the dryline season, suggesting that eastern drylines are located farther south in late fall and winter, and generally farther north in spring.

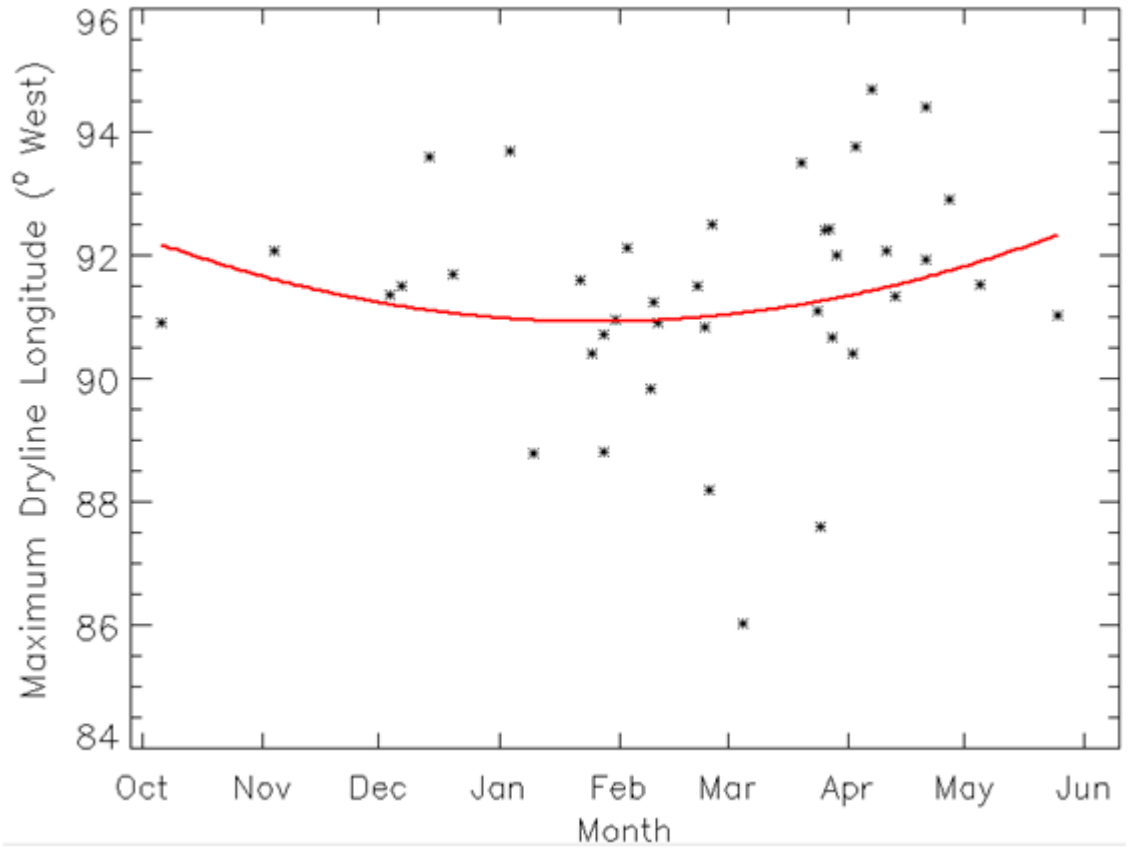

Figure 4.4a: Maximum observed dryline longitude by month. Parabolic line of best fit overlaid in red.

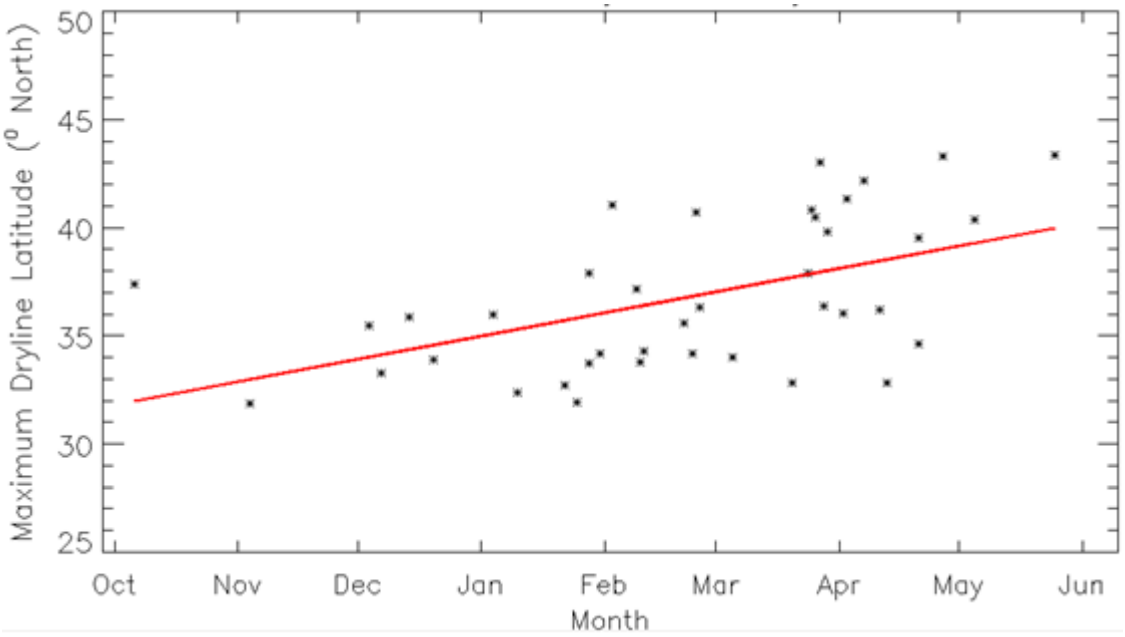

Figure 4.4b: Maximum observed dryline latitude by month. Linear line of best fit overlaid in red.

The shift in eastern dryline location throughout the season is likely due to the northward shift of the polar jet. In order for drylines to move relatively far east, there needs to be high westerly momentum mixed down to the surface. When the jet is located farther south, there is more westerly momentum available to be mixed down to the surface, resulting in drylines moving farther east. Once the polar jet retreats to the north, there is significantly less strong westerly momentum available to mix down to the surface, resulting in drylines that tend to stay farther west. The northward progression in the location of drylines also coincides with the northward retreat of associated surface cyclones. Since eastern drylines occur under very active synoptic patters and are strongly tied to a surface cyclone (more thoroughly discussed in Chapter 6), it makes sense that their location would shift northward through the spring as the typical path of surface cyclones shifts northward (Dos Santos Mesquita et al. 2008). By this reasoning, it would

make sense that eastern drylines occurring in fall (while very rare) would be located farther north than drylines observed in the winter months. This study only found two drylines that occurred in the fall months, which are not enough to make any conclusions about the location of fall drylines.

250 mb jets were present to the west of the dryline for the majority of cases, with similar analysis at 850 mb indicating an anomalously strong jet there as well on eastern dryline days. However, comparisons of the strength of the upper-level jet versus the easternmost longitude of the dryline (not shown here) revealed no correlation between the two factors. That is to say that the strongest jets to the west of the dryline did not necessarily correspond to the farthest east drylines. The drylines that moved east were almost all (with the exception of one case) located equatorward of a surface cyclone ahead of the cold front. One factor that limits how far east a dryline can travel is how soon the cold front overtakes the dryline. One theory on why a stronger jet does not necessarily mean the dryline will make it farther east is that a stronger jet would also allow the cold front to move faster and potentially overtake the dryline at an earlier stage. Figure 4.5 shows the maximum observed dryline longitude versus the maximum 24 hour attendant cyclone intensity (the lowest cyclone pressure observed in the 24 hours leading up to the dryline event). There is a slight increase in the eastward location of drylines with increasing cyclone intensity, however the correlation is very weak with a coefficient of determination value of 0.02. From this analysis, a typical attendant cyclone strength or jet strength and/or location that results in drylines moving atypically eastward cannot be proposed. These events are complex and require a combination of factors which will be further examined in Chapter 4.

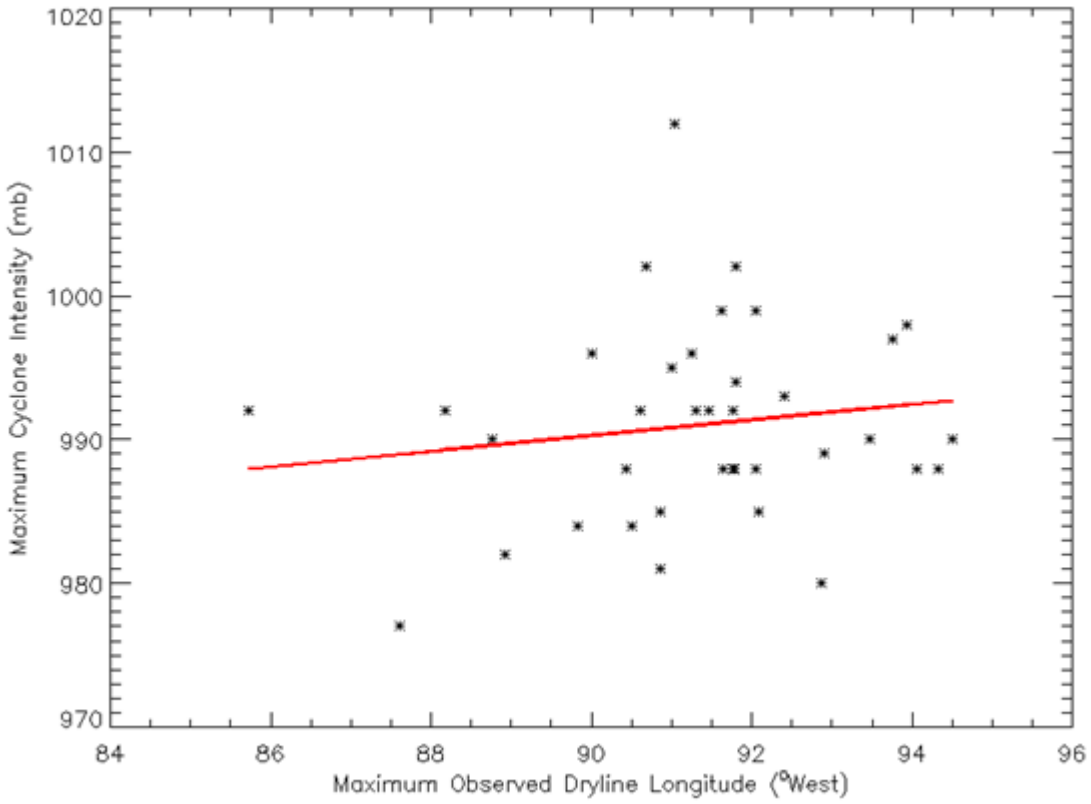

Figure 4.5: Maximum observed dryline longitude versus attendant cyclone strength

5. NOAA HYSPLIT Model Backwards Parcel Trajectories

Sixty-hour backward parcel trajectories were modeled using NOAA's HYSPLIT Lagrangian model using Global Data Assimilation System (GDAS) model data in order to identify the source of the dry air found just west of the drylines. Backward parcel trajectories for four representative different eastern dryline days are shown in Fig. 5.1. For each of the dryline days, the 60 hour backwards parcel trajectories were plotted beginning at a time when the dryline moved into the study domain. The backwards trajectories of three different points that represented mT air, cT air, and polar air are shown in Fig. 5.1. The heights indicated in Fig. 5.1 are above ground level, so the elevated terrain of the Mexican Plateau is already accounted for. The backwards parcel trajectories provide insight into the processes that resulted in cT air moving atypically eastward, specifically the roles of low-level advection versus parcels descending down from the elevated mixed layer (EML). The trajectories show that the movement of cT air eastward is often a combination of low-level advection and descent of the drier cT air from aloft, with each case being unique. In the 11 March 2011 Arkansas dryline case (Fig. 5.1a), the 200 m parcels appear to have been advected at low levels eastward into western Arkansas, while the parcels at 500 m appear to have been lofted upward to 3000 m and then descended to 500 m in the 18 hours preceding the dryline event. During a Mississippi dryline event on 24 January 2010 (Fig. 5.1b), the air parcels appear to have been advected from the Mexican Plateau eastward into Mississippi. The Iowa dryline on 17 February 2011 (Fig. 5.1c) and the 23 February 2012 Arkansas dryline (Fig. 5.1d) show similar setups to the 11 March 2011 Arkansas dryline (Fig. 5.1a), with the lower level (200 m) parcels appearing to have been advected into Iowa and the 500 m parcels

appearing to have descended 12 to 24 hours prior to the dryline event.

These backwards parcel trajectories seem to suggest that during eastern dryline events, both low-level advection of the cT air and/or descent of the EML down to the surface can be responsible for the appearance of a surface dryline. In some cases, the EML is advected to the east, and then parcels appear to generally descend to the surface on a synoptic scale. Turbulent mixing likely also contributes to the descent of the parcels, however the synoptic-scale wind flow represented in the HYSPLIT trajectories cannot resolve turbulent mixing and can only lead to conclusions about general synoptic-scale descent of parcels from aloft. In other cases, the cT air seems to originate at lower levels and is advected near the surface farther eastward. Sometimes the process that resulted in the cT air moving eastward is not as obvious, or is a combination of the two processes.

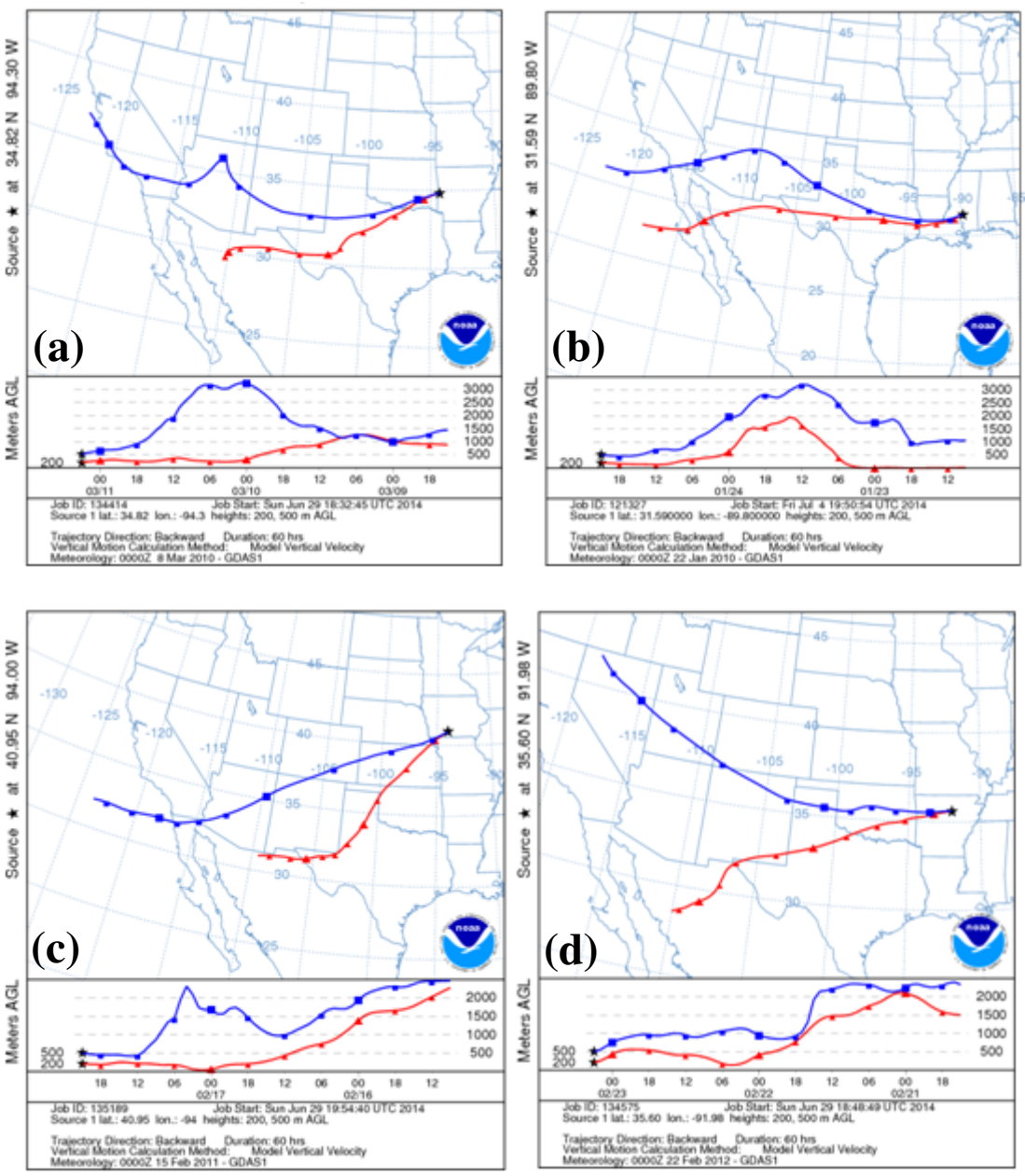

Figure 5.1: 60-hour NOAA HYSPLIT model backward parcel trajectories for parcels 200 m above ground level (red) and 500 m above ground level (blue) ending on a) 0300 UTC11 March 2010, b) 2100 UTC 24 January 2010, c) 2100 UTC17 February 2011, and d) 0300 23 February 2012. Smaller markers are plotted every 6 hours, larger markers every 24 hours.

6. Regional Composites

a) Louisiana and Arkansas Drylines

Synoptic composites were created of 25 days (listed in Table 3.2) on which drylines were analyzed in Louisiana and/or Arkansas. On Louisiana and Arkansas dryline days, mean composites of the 250 mb winds showed a jet centered over western Texas 24 hours prior to the dryline (Fig. 6.1a), northeastern Texas 12 hours prior to the dryline (Fig. 6.1c), and a large jet from mid Texas through Ohio at the time of the dryline passage (the time at which the dryline progressed the farthest east; Fig. 6.1e). Louisiana and Arkansas, the location of the drylines for these composites, was located near the center of the jet. Upper-level winds were anomalously high compared to long term means over the Midwest during the passage, and over the Mississippi River Valley and the Great Plains 12 hours and 24 hours prior to the passage respectively (Fig. 6.1b,d,f). A second, weaker jet was located over the eastern Pacific Ocean off the Pacific Northwest coast (Fig. 6.1a,c,e).

Twenty-four hours prior to the dryline passage, the 500 mb geopotential height composites show a trough over the Rocky Mountains (Fig. 6.2a). By 12 hours prior to the dryline passage, the trough has progressed to the central Plains (Fig. 6.2c), and at the time of the dryline passage the trough has slightly amplified and is located over the central Plains/upper Mississippi River Valley (Fig. 6.2e).

850 mb zonal winds on these days were anomalously positive (westerly) (up to 8 m s^{-1}) in the south-central United States leading up to the dryline time and over the southern Mississippi River Valley during the dryline event (Fig. 6.3a,c,e). There were also positive anomalies of 850 mb zonal winds (up to 8 m s^{-1}) over the eastern Pacific

Ocean off of the Pacific Northwest coast (Fig. 6.3b,d,f). Negative (northerly) 850 mb zonal wind anomalies were present over the northern Plains and northern Great Lakes states (Fig. 6.3b,d,f). 850 mb meridional winds were anomalously positive (southerly) to the east of the dryline, and anomalously negative to the west of the dryline (Fig. 6.4b,d,f). Strong southerlies to the east of the dryline are virtually always observed on dryline days (Hoch and Markowski 2005), as they advect mT air onto the continent. 850 mb meridional winds are likely indicative of a low-level jet (LLJ) in the cyclone's warm sector. 850 mb temperatures were consistent with the upper-air wind pattern, with anomalously cold temperatures observed in the western United States and anomalously warm temperatures observed in the eastern United States (Fig. 6.5).

Analysis of the sea level pressure composites reveals a mean surface cyclone located over the southern/central Plains prior to the dryline passage and located over the Midwest at the time of the dryline passage (Fig. 6.6a,c,e). The surface cyclone has negative anomalies of over 14 mb (Fig. 6.6b,d,f). A secondary, weaker surface cyclone is located off the Pacific Northwest (Fig. 6.6a,c,e).

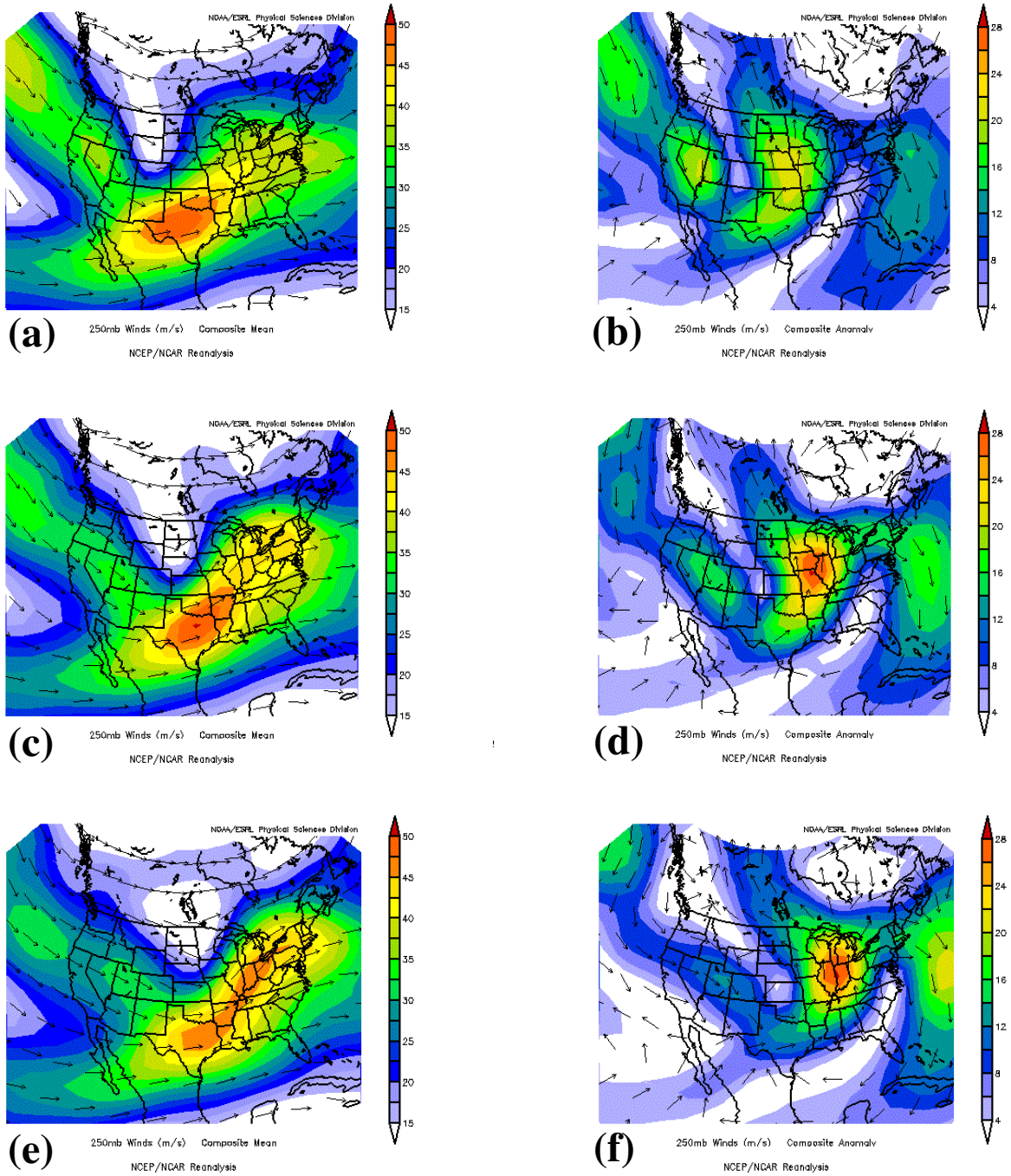

Figure 6.1: 250 mb vector wind (m s^{-1}) composites for Louisiana and Arkansas dryline days. a) composite mean 24 hours prior to event, b) composite anomaly 24 hours prior to event, c) composite mean 12 hours prior to event, d) composite anomaly 12 hours prior to event, e) composite mean at time of event, f) composite anomaly at time of event.

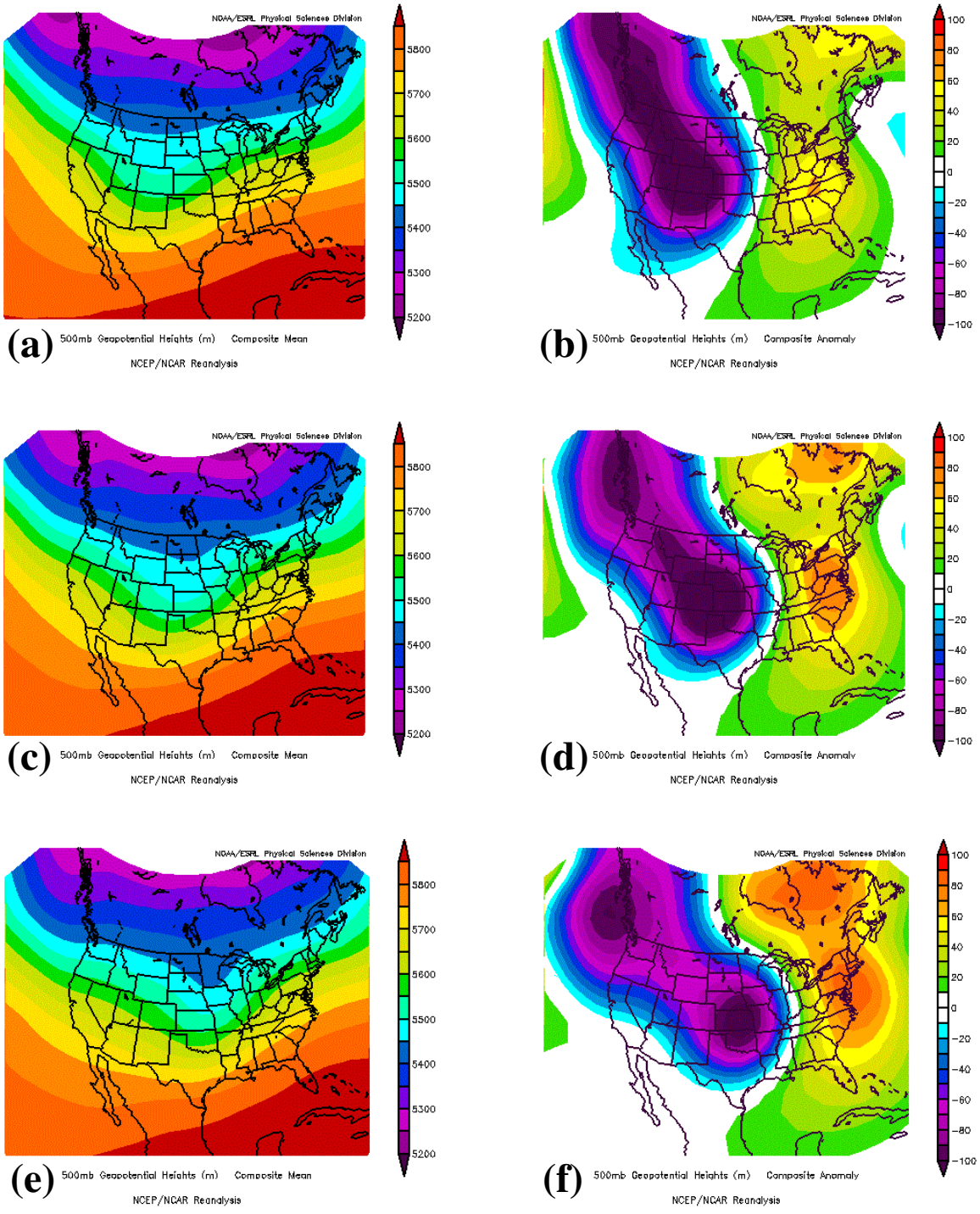

Figure 6.2: As in Figure 6.1, except 500 mb geopotential height (m) composites for Louisiana and Arkansas dryline days.

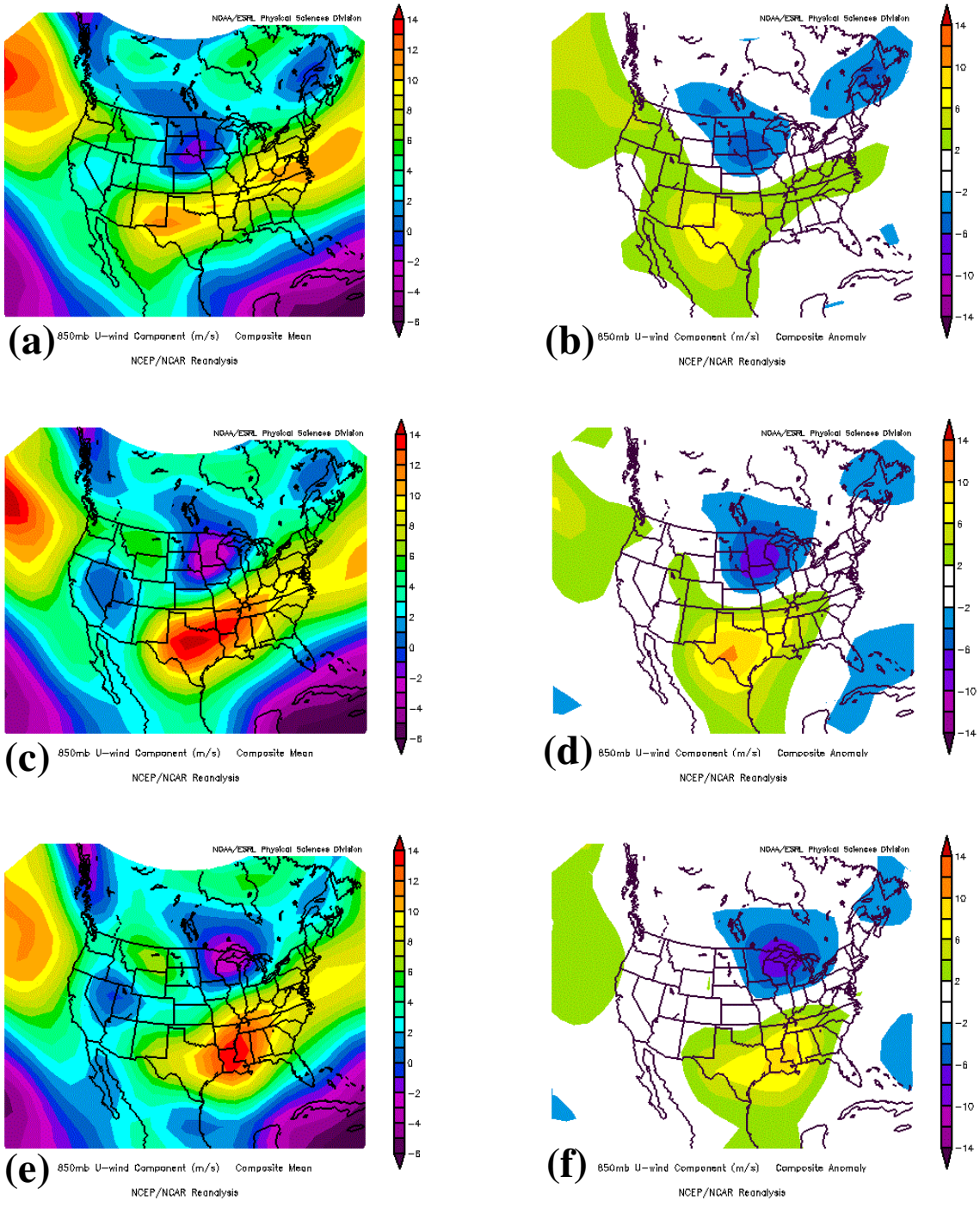

Figure 6.3: As in Figure 6.1, except 850 mb zonal wind (m s^{-1}) composites for Louisiana and Arkansas dryline days.

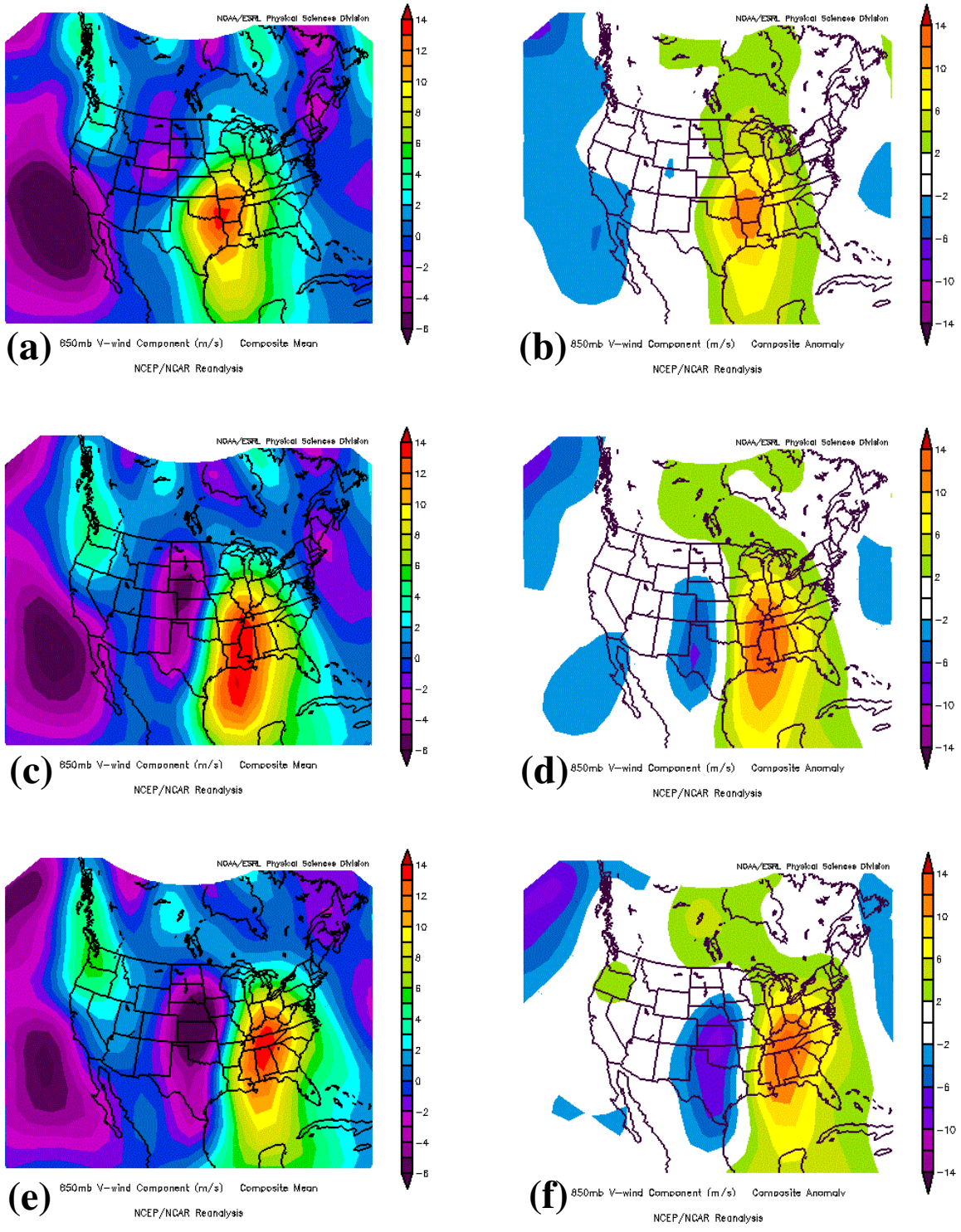

Figure 6.4: As in Figure 6.1, except 850 mb meridional wind (m s^{-1}) composites for Louisiana and Arkansas dryline days.

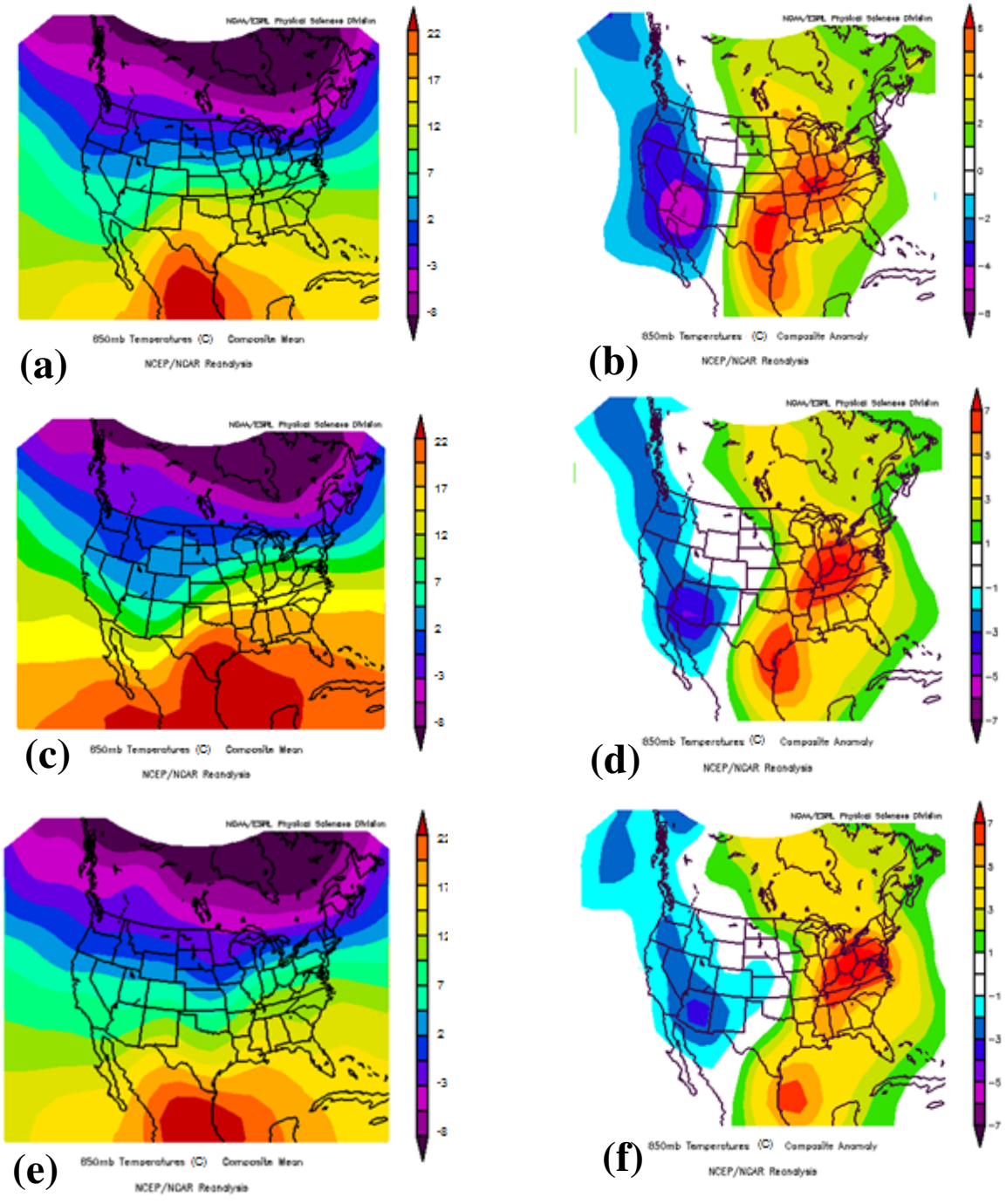

Figure 6.5: As in Figure 6.1, except 850 mb temperature (°C) composites for Louisiana and Arkansas dryline days.

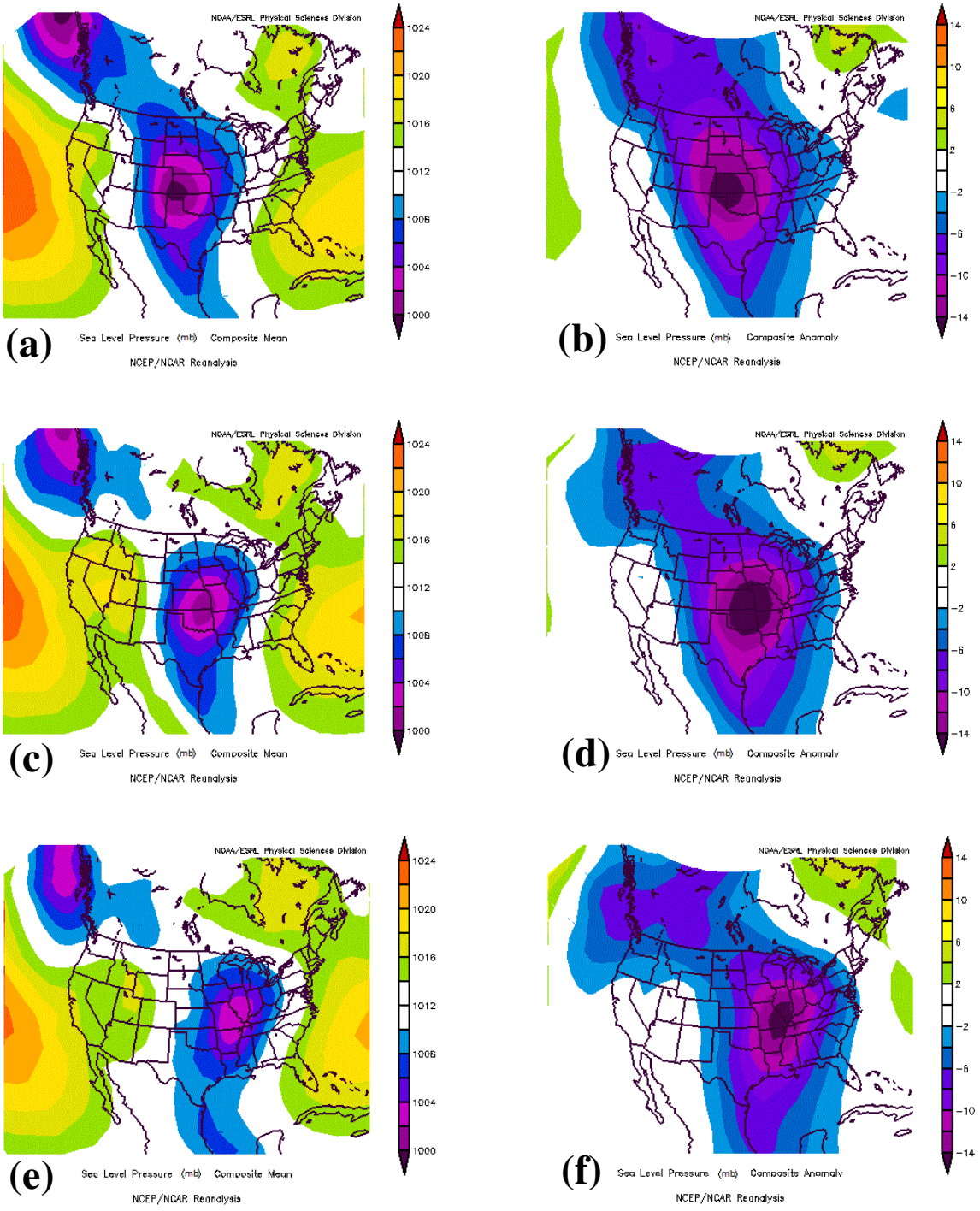

Figure 6.6: As in Figure 6.1, except sea level pressure (mb) composites for Louisiana and Arkansas dryline days.

b) Missouri, Iowa, and Illinois Drylines

There were 16 days (listed in Table 3) on which a dryline was analyzed in Missouri, Iowa, and/or Illinois. Only two of these days, 19 October 2004 and 11 February 2013, were also included in the Louisiana and/or Arkansas composites. Twelve and twenty four hours prior to the dryline passage, a 250 mb jet of similar magnitude as observed in the Louisiana/Arkansas composites was located over western Texas and New Mexico with positive upper-level wind anomalies located over the central/northern Plains (Fig. 6.7a,b,c,d). At the time of the dryline passage, the upper-level jet had progressed slightly eastward and was located over Texas and Oklahoma, with the drylines located in the left exit region of the jet (Fig. 6.7d). Upper-level winds were anomalously strong over the upper Mississippi River Valley during the dryline passage (Fig. 6.7f).

500 mb geopotential heights composites reveal a trough located over the Rockies prior to the dryline passage and the northern Plains during the dryline passage (Fig. 6.8a,c,d). The central and western portion of the United States is dominated by troughing with negative 500 mb geopotential height anomalies of over 100 m 24 hours prior to the passage and around 100 m during the dryline passage (Fig. 6.8b,d,f). The eastern portion of the United States is dominated by 500 mb ridging with positive anomalies of up to 100 m observed (Fig. 6.8b,d,f). The shortwave trough observed in the Missouri, Iowa, and Illinois dryline composites was of similar magnitude to the shortwave observed in the Louisiana and Arkansas composites and had the same slight negative tilt, however it was slightly more amplified and was located farther north.

Like the Louisiana and Arkansas drylines, the 850 mb winds for Missouri, Iowa,

and Illinois drylines had positive zonal anomalies to the southeast of the drylines (up to 10 m s^{-1}) and negative zonal anomalies (up to -6 m s^{-1}) to the north of the dryline, over the northern Plains and southern Manitoba (Fig. 6.9b,d,f). The meridional 850 mb wind anomalies were positive (up to 14 m s^{-1}) to the east of the dryline, likely indicating the presence of a LLJ, and slightly negative (up to -6 m s^{-1}) to the west (Fig. 6.10b,d,f). On these days, relatively strong southerlies over a large portion of the Mississippi River Valley (Fig. 6.10a,c,e) aided in transporting the Gulf of Mexico moisture northward into Missouri, Iowa, and Illinois. 850 mb temperature mean composites (Fig. 6.11a,c,e) showed a slightly stronger temperature gradient located to the west of Missouri, Iowa, and Illinois drylines than was observed in the Louisiana and Arkansas drylines. The temperature anomalies (Fig. 6.11b,d,f) were consequently 2 to 3 degrees stronger than those observed in the Louisiana and Arkansas composites.

A composite pattern like the one in Fig. 6.12 suggests that tendency for cyclones to be located over the central US for eastern dryline days. The mean cyclone observed is similar in intensity to the mean cyclone observed in association with Louisiana and Arkansas drylines, however the mean cyclone for Missouri, Iowa, and Illinois drylines is generally located farther north. There is also a weak anomalous area of high pressure located over the eastern Pacific and the western Atlantic on these days (Fig. 6.12b,d,f).

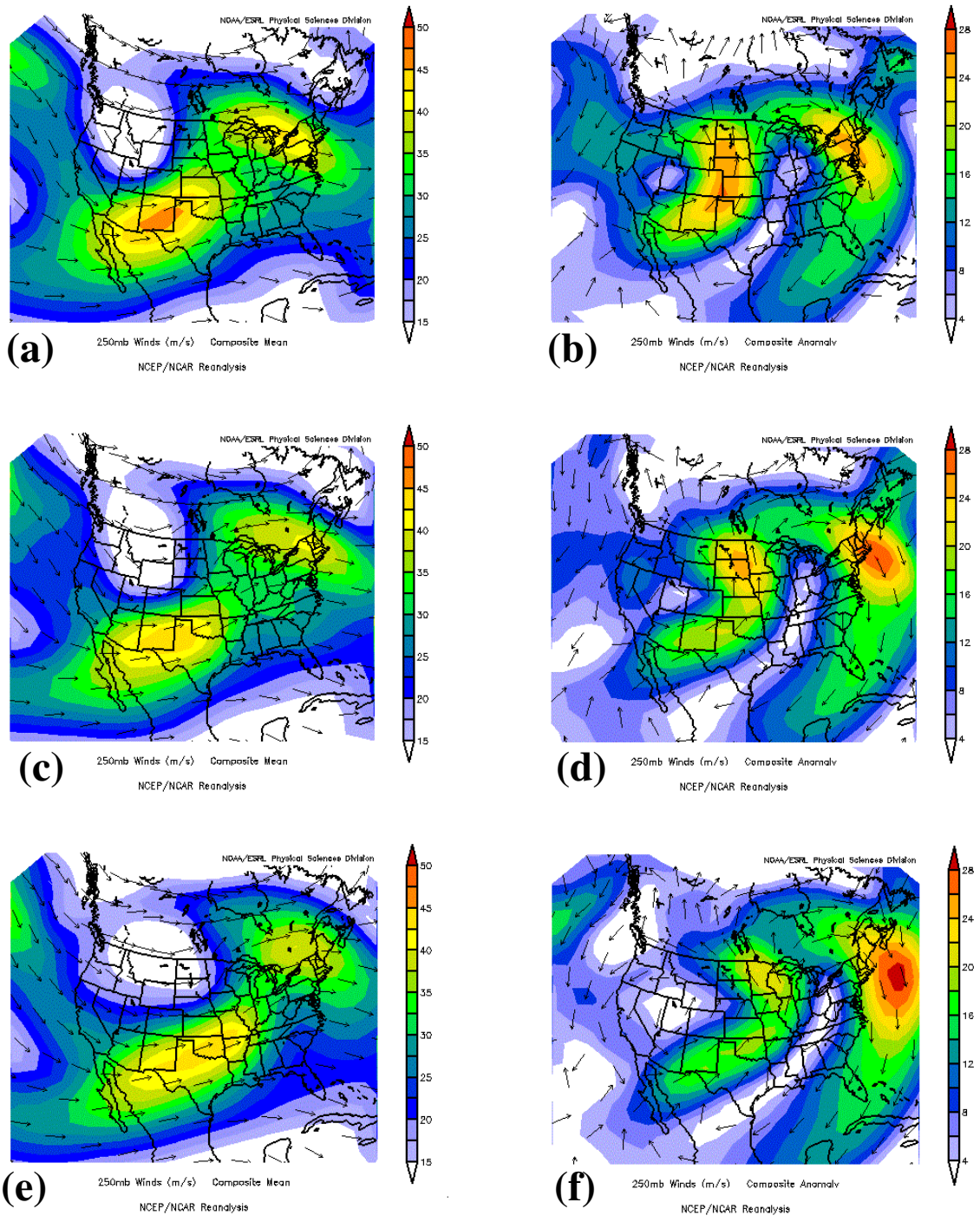

Figure 6.7: 250 mb vector wind (m s^{-1}) composites for Missouri, Iowa, and Illinois dryline days. a) composite mean 24 hours prior to event, b) composite anomaly 24 hours prior to event, c) composite mean 12 hours prior to event, d) composite anomaly 12 hours prior to event, e) composite mean at time of event, f) composite anomaly at time of event.

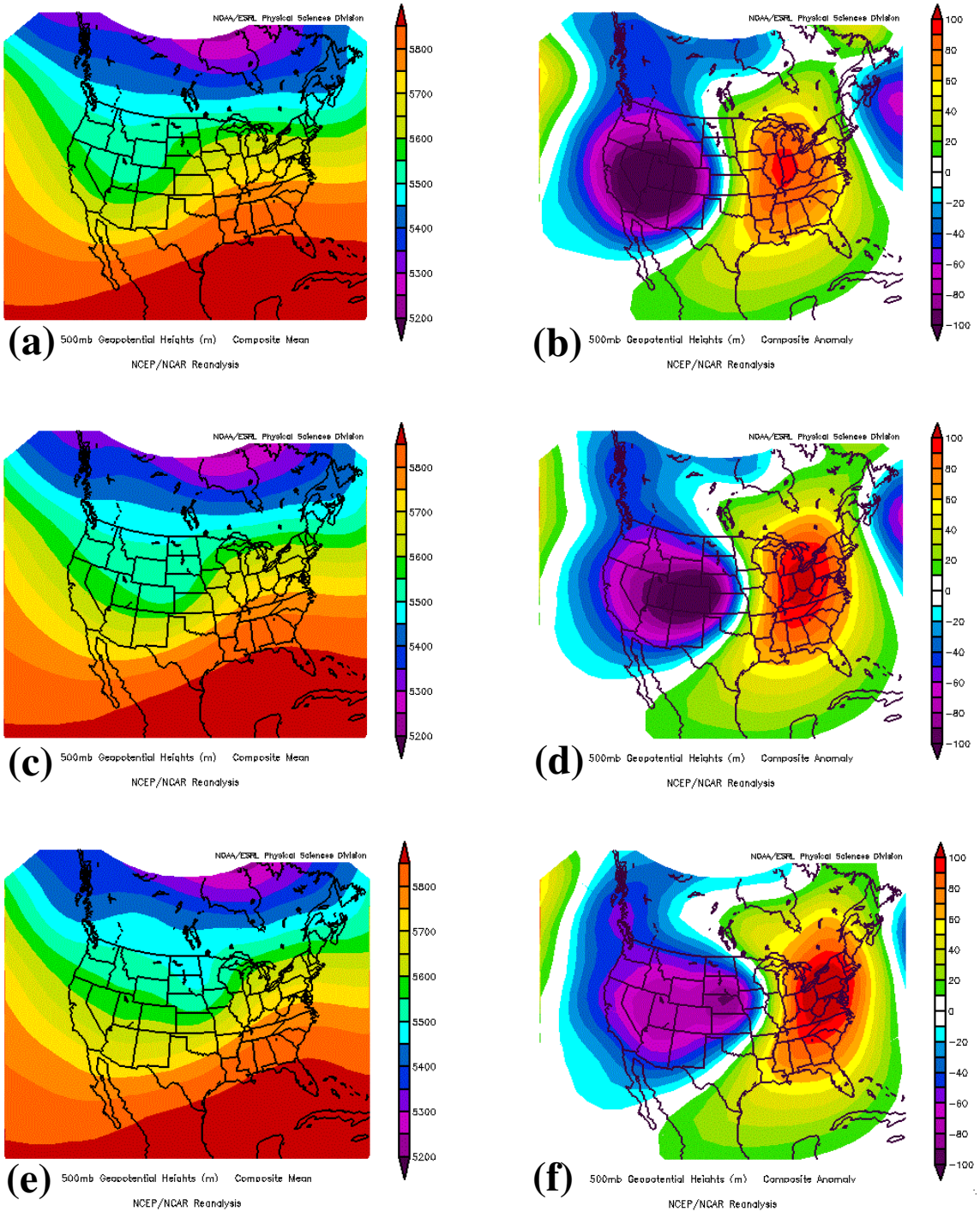

Figure 6.8: As in Figure 6.7, except 500 mb geopotential height (m) composites for Missouri, Iowa, and Illinois dryline days.

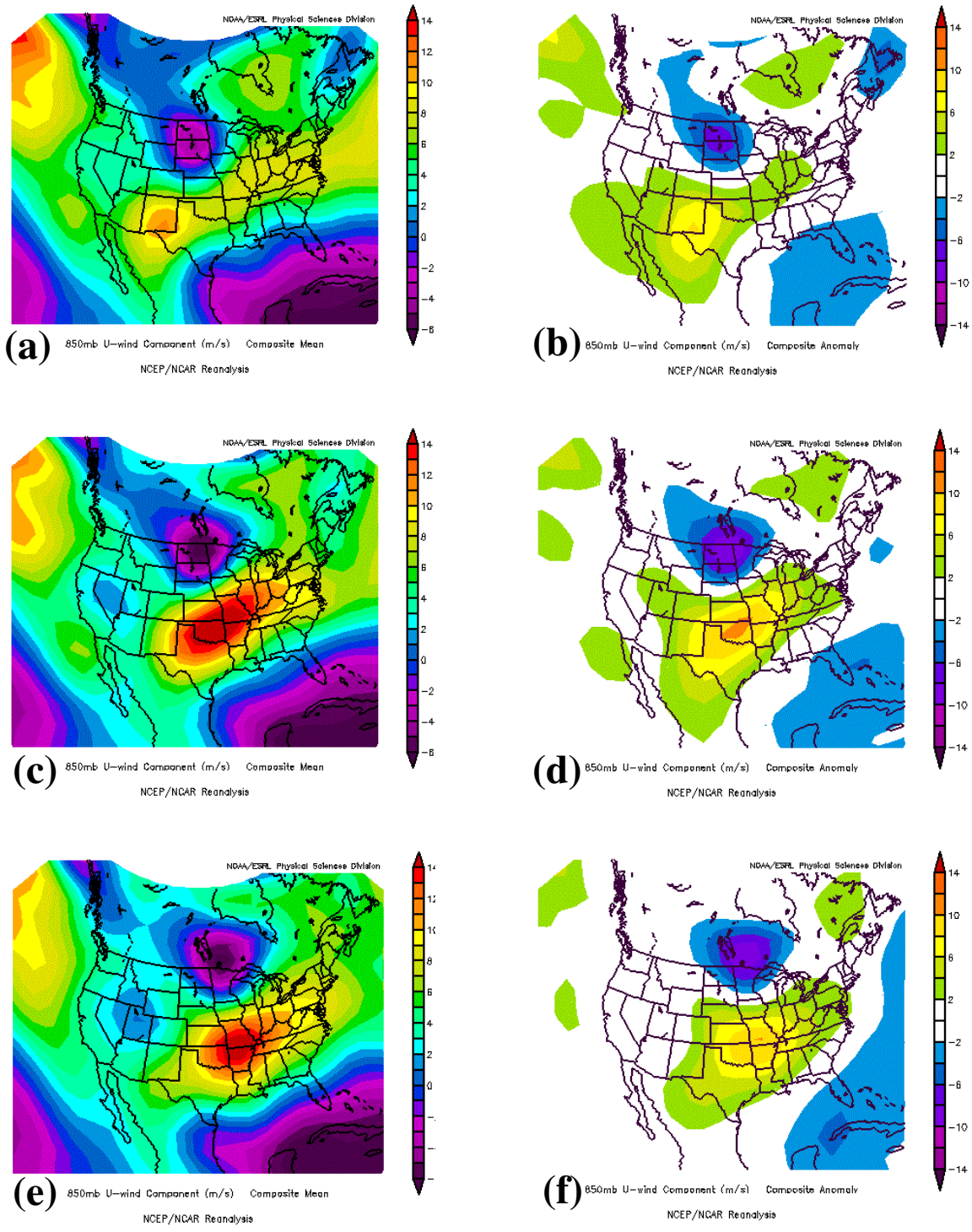

Figure 6.9: As in Figure 6.7, except 850 mb zonal wind (m s^{-1}) composites for Missouri, Iowa, and Illinois dryline days.

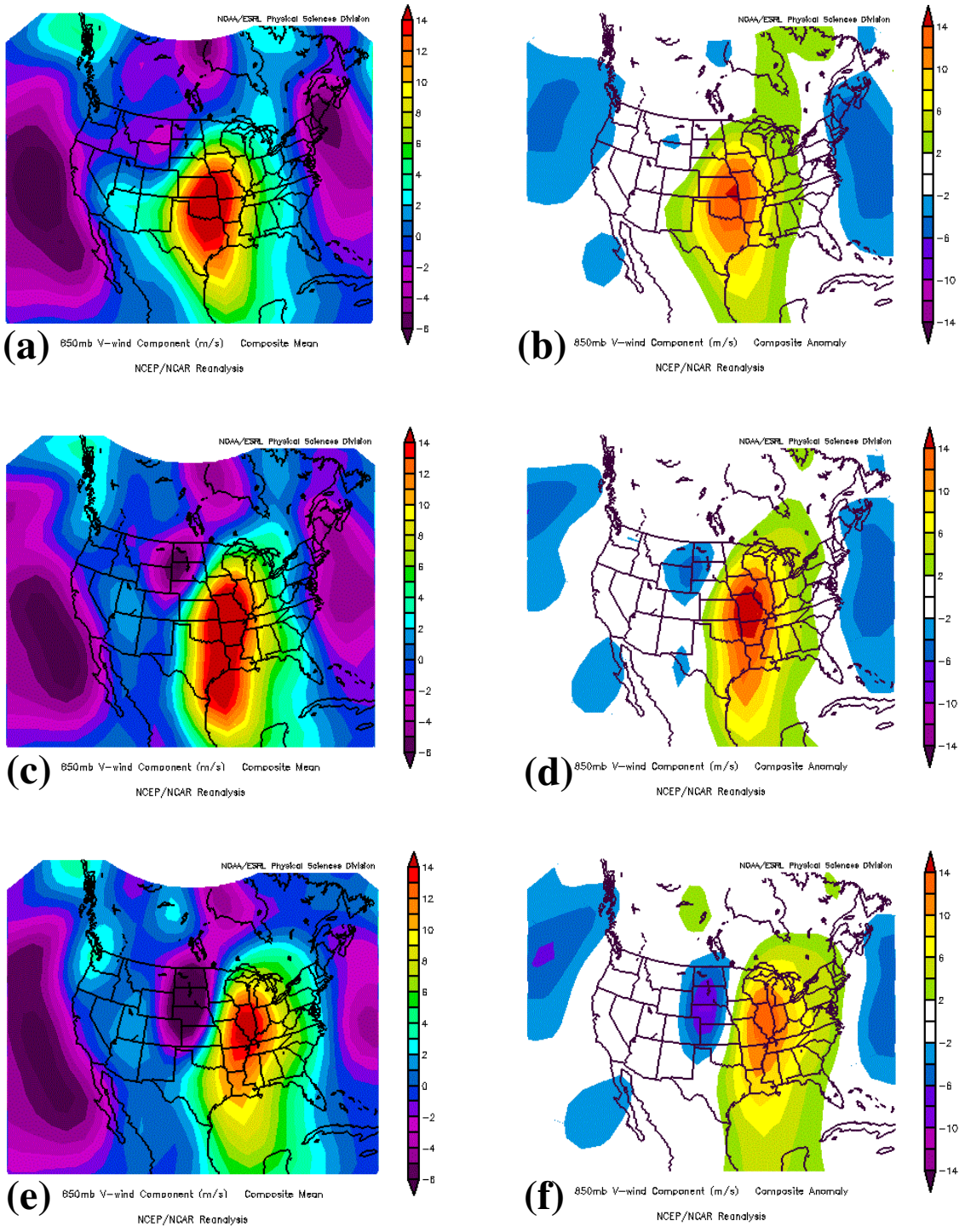

Figure 6.10: As in Figure 6.7, except 850 mb meridional wind (m s^{-1}) composites for Missouri, Iowa, and Illinois dryline days.

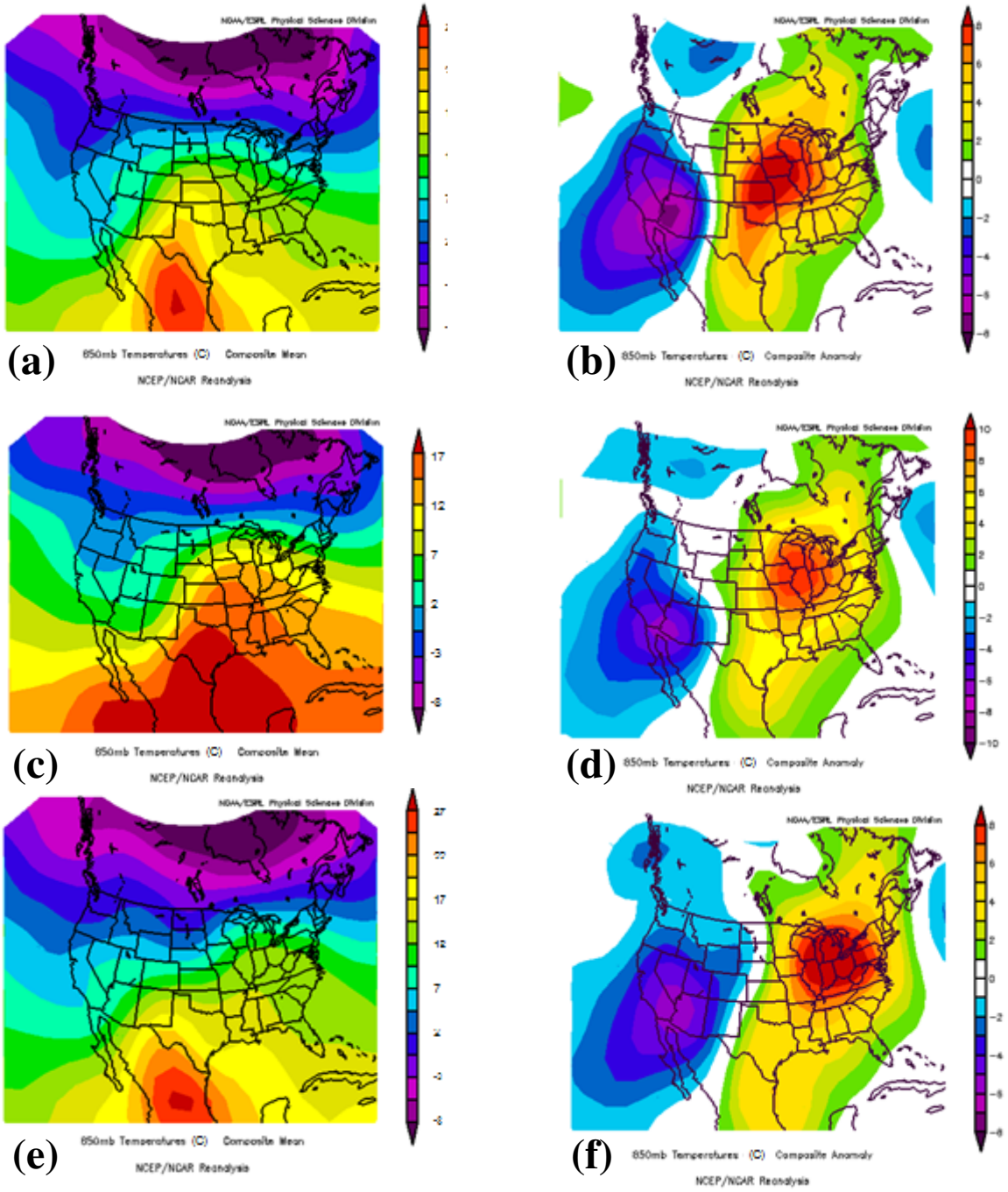

Figure 6.11: As in Figure 6.7, except 850 mb temperature (°C) composites for Missouri, Iowa, and Illinois dryline days.

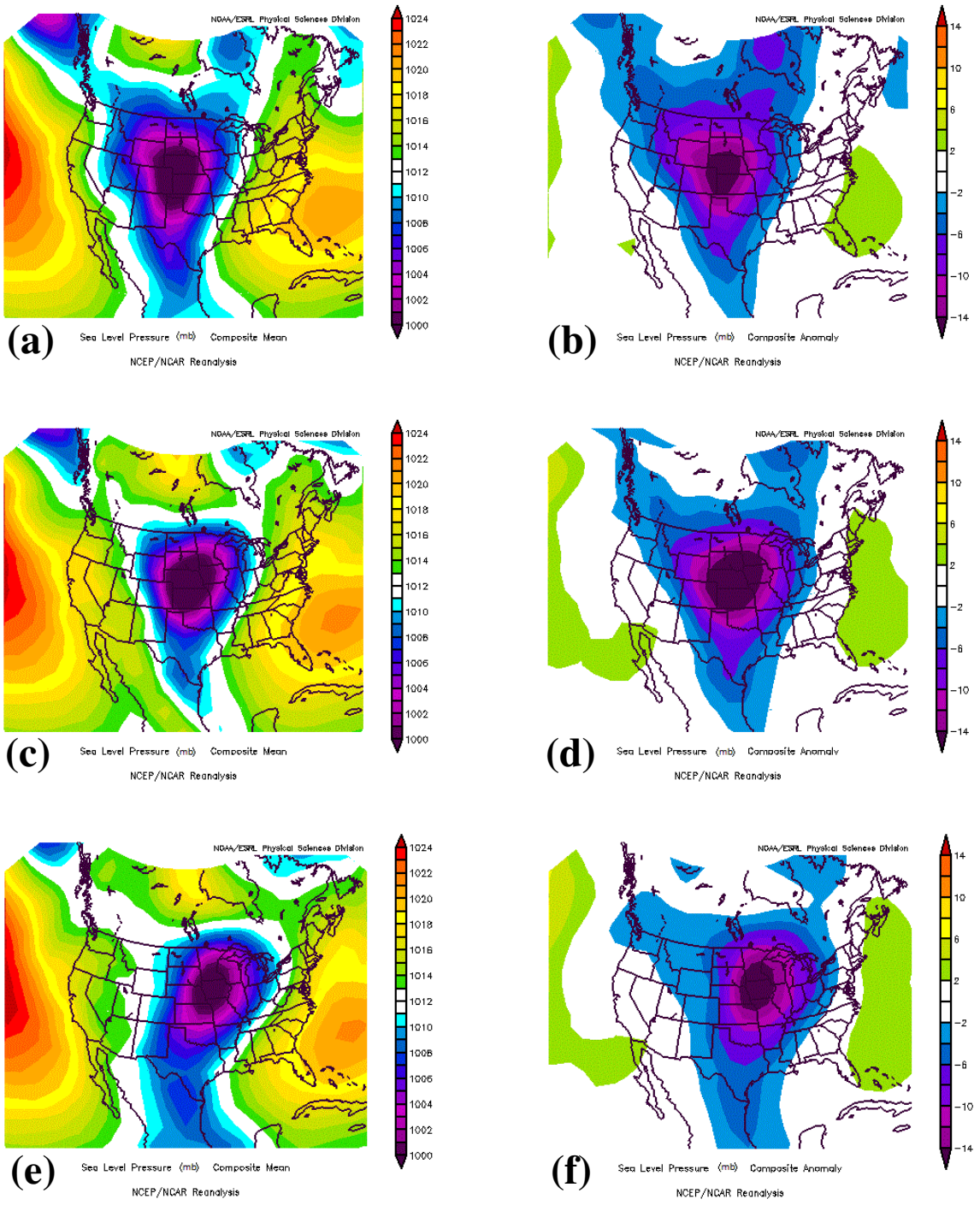

Figure 6.12: As in Figure 6.7, except sea level pressure (mb) composites for Missouri, Iowa, and Illinois dryline days.

c) Alabama and Mississippi Drylines

Composites were created of the synoptic conditions on the days of three dryline passages (days listed in Table 4) in Mississippi and Alabama. Drylines that progressed as far as Alabama or Mississippi were marked by a very strong 250 mb jet over the southeastern United States (Fig. 6.13). Twenty four hours prior to the dryline moving into Mississippi or Alabama, the jet was located quite far south over northern Mexico and 12 hours prior to the dryline passage, the composite mean jet maximum was located over eastern Texas and Louisiana (Fig. 6.13a,c). A jet of over 60 m s^{-1} was centered over Mississippi and Alabama at the time of the mean dryline passage with large 250 mb wind speed anomalies over the Midwest (Fig. 6.13e,f). The jet observed in these composites was 10 to 20 m s^{-1} stronger than the composite jet observed in the other two regional composites.

A composite of the 500 mb geopotential heights (Fig. 6.14) showed a large negatively-tilted trough of higher amplitude and lower heights than the mean shortwaves observed in the other regional composites. 24 hours prior to the passage, the mean trough was located over the Rocky Mountains and 12 hours prior to the passage, the trough was located over the central United States (Fig. 6.14a,c). The 500 mb heights were over 200 m lower than average along the trough 12 and 24 hours prior to the dryline event (Fig. 6.14,b,d). At the time of the dryline passage, the trough was located over the central United States and the Mississippi River Valley (Fig. 6.14e). During and prior to the eastern dryline event, the northeastern United States and the Hudson River Valley were characterized by mid-level ridging (Fig. 6.14), which likely contributed to the deepening

of the upstream trough and the upstream negative height anomalies. A unique feature observed in the 500 mb mean composites to the Mississippi and Alabama drylines was a closed low in the 24 and 12 hours prior to the dryline event (Fig. 6.14a,e). Twenty four hours before the dryline was analyzed, this closed low was located over the Four Corners region. Twelve hours before the event, the closed low had progressed to western Oklahoma, and by the time of the dryline event, the low was no longer closed.

The Alabama and Mississippi drylines days had relatively strong positive 850 mb zonal winds over the south-central United States leading up to the eastern dryline event and 850 mb zonal winds of up to 14 m s^{-1} over the southern Mississippi River Valley on the day of the dryline (Fig. 6.15a,c,e). Similar to that of the drylines that occurred in the Mississippi River Valley, 850 mb meridional winds were strongly positive (up to 20 m s^{-1}) to the east of the dryline and negative to the west of the dryline (Fig. 6.16a,c,e). The Alabama and Mississippi 850 mb zonal (Fig. 6.15b,d,f) and meridional (Fig. 6.16b,d,f) wind anomalies were about 5 m s^{-1} stronger than the anomalies observed in the drylines farther west. 850 mb temperature anomalies (Fig. 6.17) were also stronger in these drylines than were observed in the drylines farther west. This is consistent with a more amplified upper and mid-level air patterns observed in these cases and allowed for more intense cyclones to develop.

Mean sea level pressure composites showed a deep surface cyclone located north of the dryline (Fig. 6.18a,c,d). It had a negative sea level pressure composite anomaly of over 20 mb over the Midwest at the time of the passage and over the Plains prior to the dryline passage (Fig. 6.18b,d,f). This mean surface cyclone had a negative pressure anomaly of about 5 mb greater than the negative sea level pressure anomaly observed in

the other regional composites, indicating a more intense cyclone.

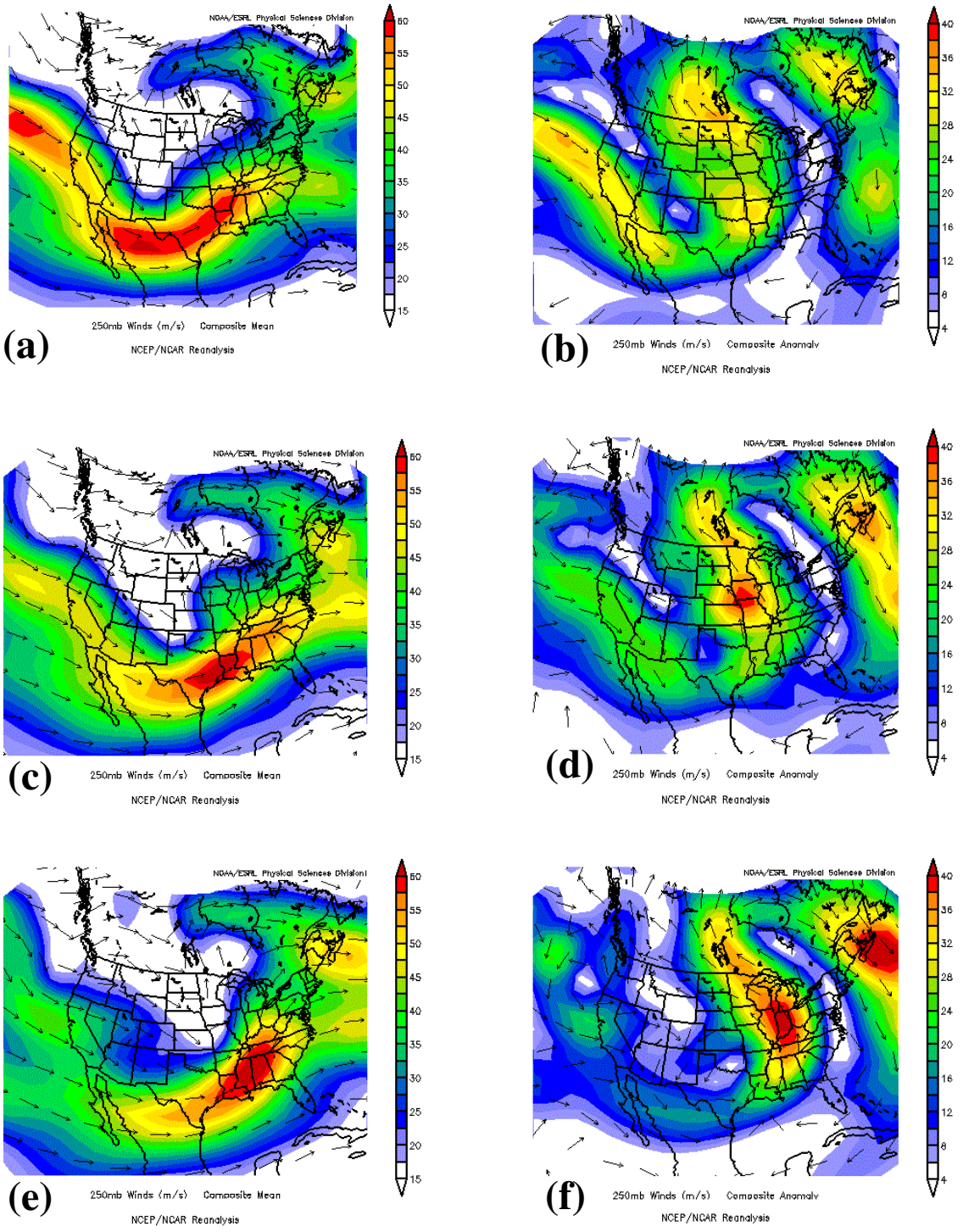

Figure 6.13: 250 mb vector wind (m s^{-1}) composites for Alabama and Mississippi dryline days. a) composite mean 24 hours prior to event, b) composite anomaly 24 hours prior to event, c) composite mean 12 hours prior to event, d) composite anomaly 12 hours prior to event, e) composite mean at time of event, f) composite anomaly at time of event.

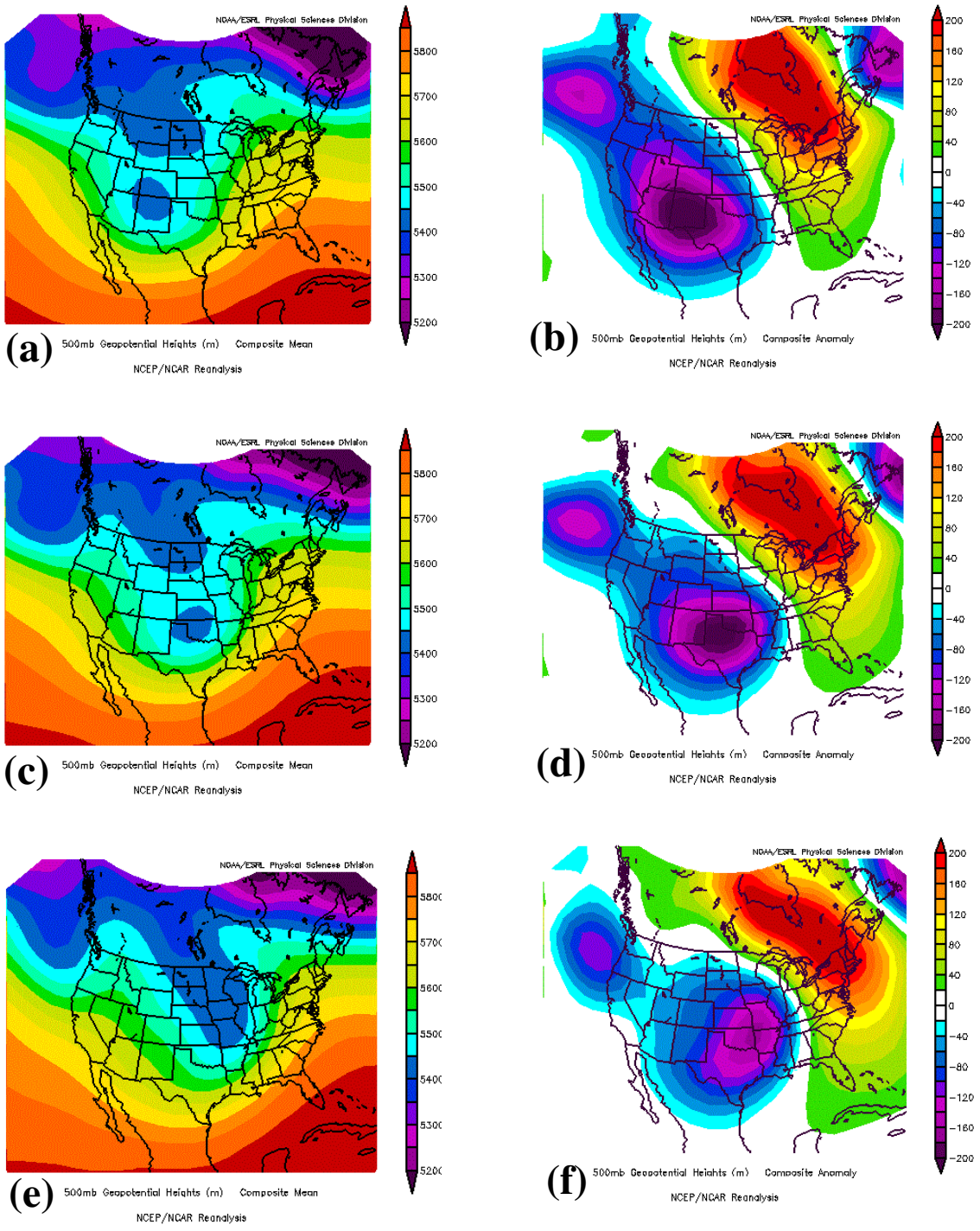

Figure 6.14: As in Figure 6.13, except 500 mb geopotential height (m) composites for Alabama and Mississippi dryline days.

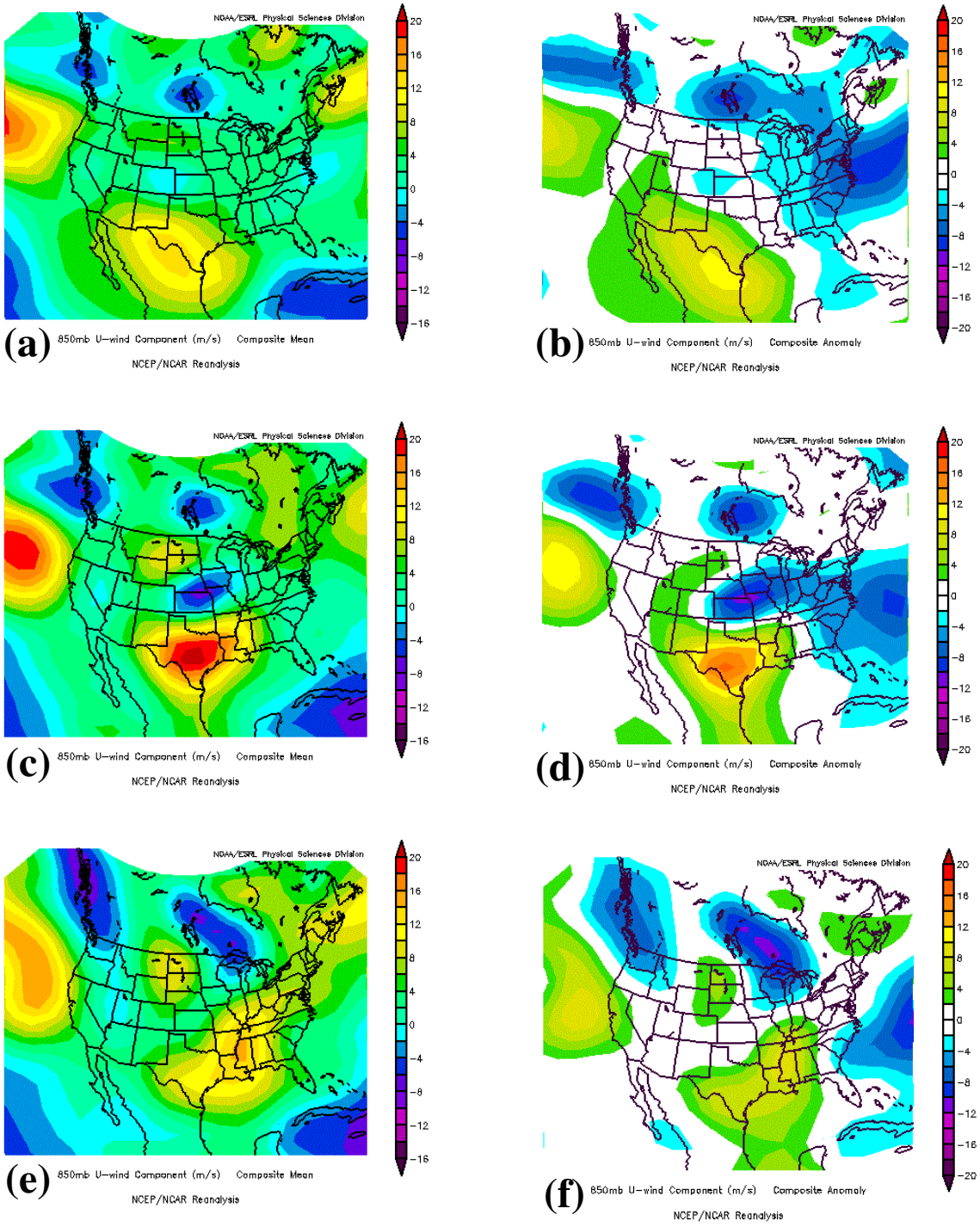

Figure 6.15: As in Figure 6.13, except 850 mb zonal wind (m s^{-1}) composites for Alabama and Mississippi dryline days.

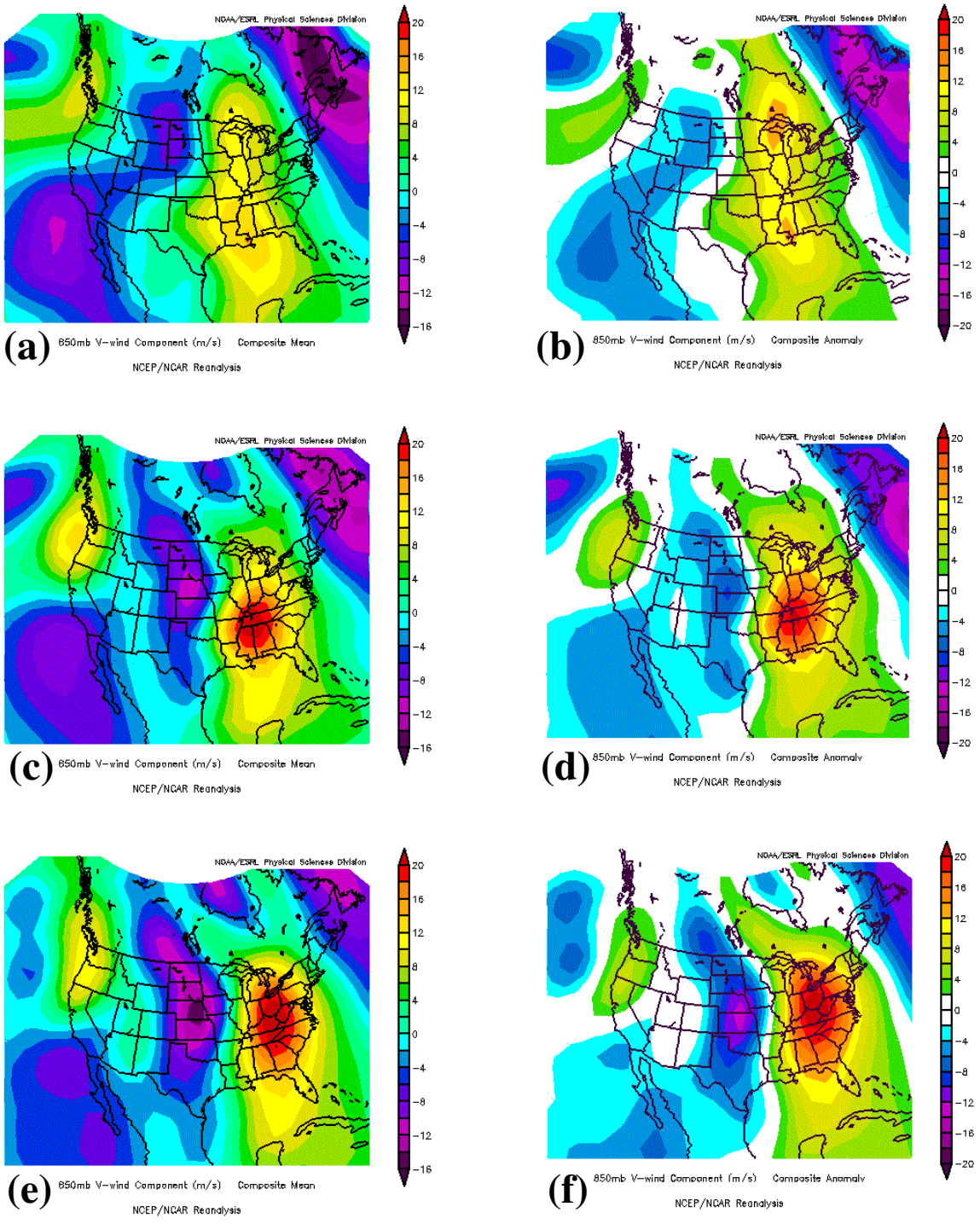

Figure 6.16: As in Figure 6.13, except 850 mb meridional wind (m s^{-1}) composites for Alabama and Mississippi dryline days.

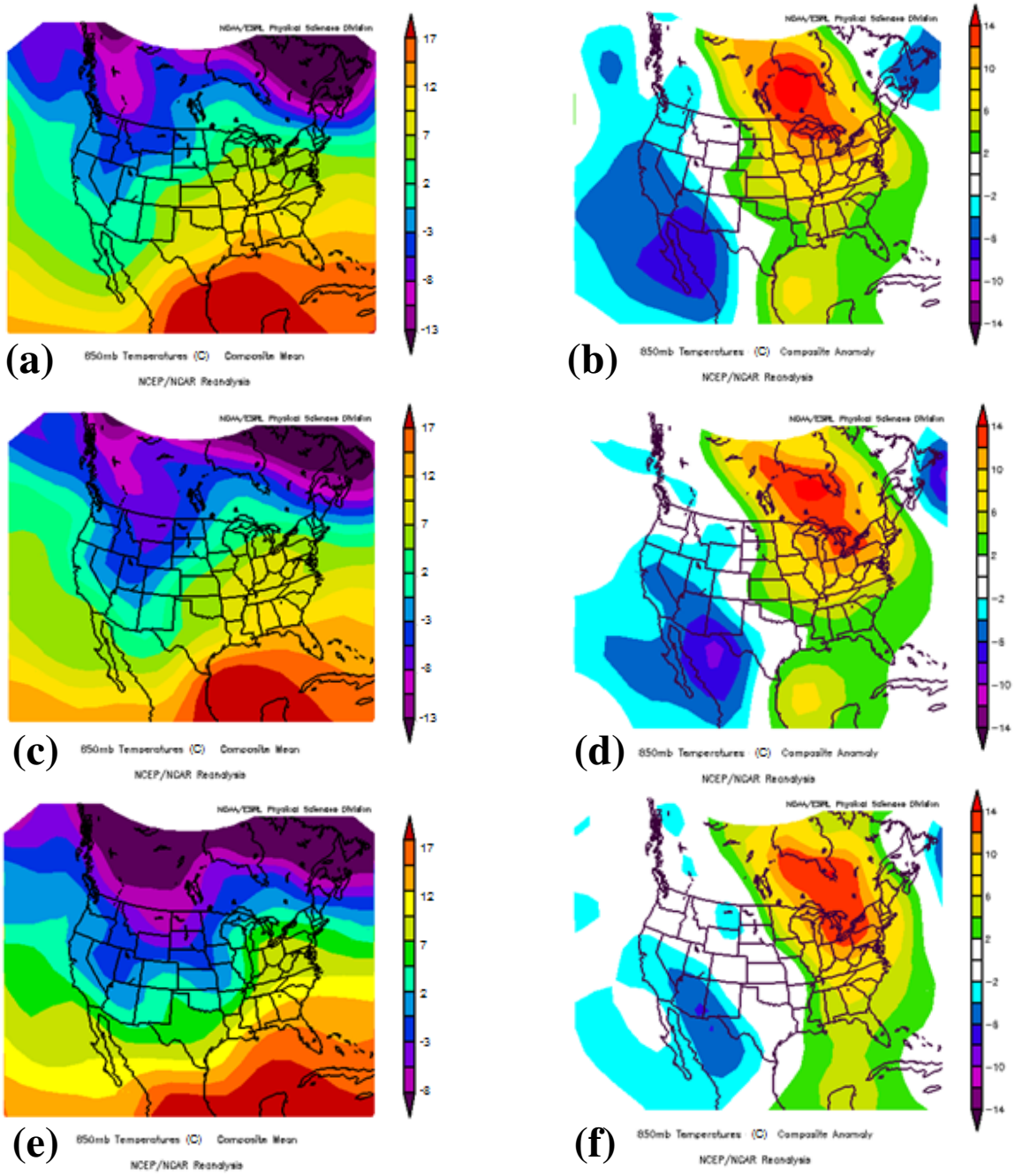

Figure 6.17: As in Figure 6.13, except 850 mb temperature (°C) composites for Alabama and Mississippi dryline days.

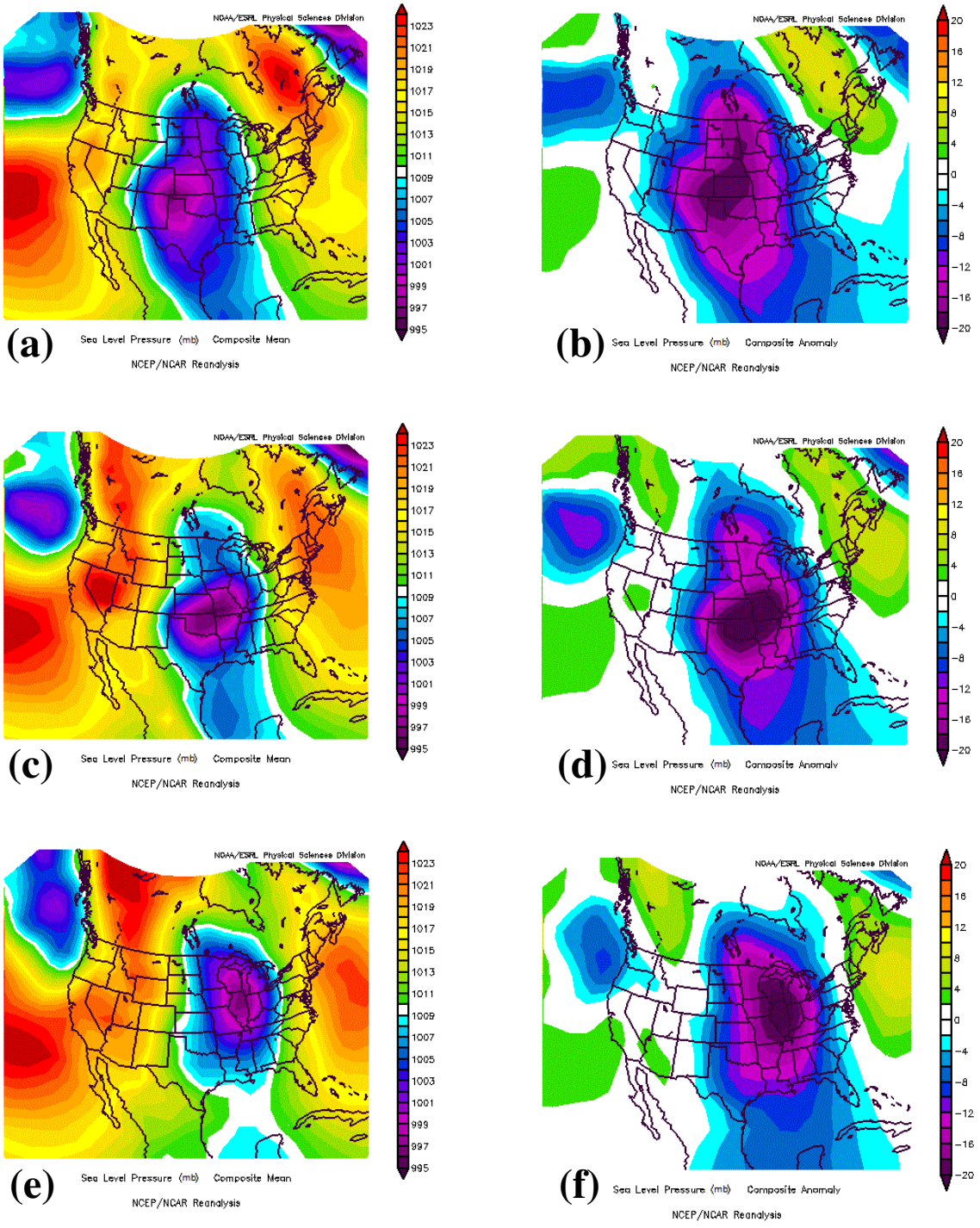

Figure 6.13: As in Figure 6.13, except sea level pressure (mb) composites for Alabama and Mississippi dryline days.

Caution should be applied when comparing the results of the regional composites. Due to the constraints of the numbers and locations of drylines identified in this study, different numbers of cases were used in creating the regional composites. 25 days were included in the composites of Louisiana and/or Arkansas drylines, 16 days were included in the composites of Missouri, Iowa, and/or Illinois drylines, and only 3 days were included in the composites of Alabama and/or Mississippi drylines. While it does appear that the synoptic conditions were slightly more active on days when drylines moved into Alabama and Mississippi, three cases cannot support climatological conclusions. However, the three cases indicate preliminary patterns which should be investigated further.

The composites for all three regional dryline events revealed a common synoptic setup for eastern drylines with minor variations in the location and strength of the synoptic features by region. The upper-air pattern on eastern dryline days is very amplified with relatively large zonal and meridional anomalies. The composites showed that eastern drylines are associated with the polar jet dipping into the southern United States with an upper-level jet over or just to the west of the location of the dryline. Often, the polar jet merged with the subtropical jet to the east or the southeast of the dryline location. In order for drylines to move east of their typical Great Plains domain, strong westerly momentum needs to be present to the west of the dryline. Jets at different levels provide this westerly momentum that is then mixed down to the surface and advects the dryline eastward. For drylines that moved into the Mississippi River Valley region (Iowa, Missouri, Illinois, Arkansas, and Louisiana) strong jet were observed to the west of the dryline (up to 50 m s^{-1}; Fig. 6.1 and Fig. 6.7). However, drylines that made it even

farther east into the southeastern United States (Mississippi and Alabama), were marked by jets of even strong magnitude (greater than 60 m s^{-1}; Fig. 6.13). While the polar jet stream dips into the southern part of the United States to the west of the dryline, it retreats slightly northward to the east of the dryline, resulting in large upper-air southerly flow anomalies over the Midwest. A relatively amplified upper-air pattern like the ones seen on these dryline days would support large low-level baroclinicity and intense cyclogenesis. 850 mb temperature mean composites indeed show the strong temperature gradients that fueled the intense surface cyclones which played a large role in moving these drylines atypically eastward.

500 mb geopotential height patterns for Mississippi River Valley drylines were relatively similar, with shortwave troughs present to the northwest of the dryline including negative height anomalies of just over 100 m. However, drylines that moved into Mississippi and Alabama were associated with a negatively-tilted trough with much larger negative 500 mb geopotential height anomalies than other eastern drylines. The negatively-tilted trough likely supported the stronger surface cyclone and increased baroclinicity, leading to an increase in the low-level wind field. The negatively-tilted trough likely also supported strong upper-level divergence over the surface low, allowing for increased ascent over the region.

The negative mean composite anomalies for drylines that moved into Mississippi and Alabama were up to 200 m (100 m greater anomalies than drylines that only moved into the Mississippi River Valley). This mid-level short-wave feature that was associated with the eastern drylines is indicative of synoptically-active drylines (Hane 2004), and likely plays a large role in advecting the dryline so far east.

The eastern drylines were all associated with a surface cyclone to the north of the boundary, consistent with the findings of past studies (e.g., Hoch and Markowski 2005). Like the other synoptic features, the surface cyclone was anomalously stronger (6 mb mean composite negative anomaly) for the Mississippi and Alabama drylines than was present for the drylines in the western part of the study's domain. The 850 mb winds were consistent with a surface cyclone, with positive zonal anomalies observed to the south of the cyclone and negative zonal anomalies to the north, and positive meridional anomalies to the east of the dryline/surface cyclone and negative meridional anomalies to the west. While the location of the 850 mb maximum winds shifted north or south slightly for drylines in Louisiana, Arkansas, Missouri, Iowa, or Illinois, the magnitude was roughly the same. However, the magnitudes of the 850 mb wind maxima were about 5 m s^{-1} greater for drylines that occurred in Alabama and Mississippi than for drylines that occurred to the west. This is consistent with the results of Hoch and Markowski (2005), who showed that Great Plains drylines moved farther east with increasing westerly momentum between 850 and 500 mb. This study shows that this relationship between low-level westerly winds and maximum dryline longitude translates to eastern drylines as well. Additional composites of vector winds at different levels (not shown here) revealed the presence of a composite low-level jet to the east of the location of the dryline that was present for each of the regional categories. The low-level jet was generally strongest 12 hours before the event and advected large amounts of mT air into the warm sector of the cyclone, allowing for an enhanced moisture gradient across the dryline.

Composites of these drylines are similar to the composites of "strong drylines" created by Schultz et al. (2007). Both their composites and the composites of eastern

drylines were marked by a jet maximum of over 25 m s^{-1} over the eastern Pacific Ocean, a 500 mb shortwave trough to the northwest of the dryline, and a composite surface cyclone with central pressure less than 1004 mb to the north of the dryline (Schultz et al. 2007). Their study illustrated the importance of strong large-scale confluence from lee-troughing in creating very strong synoptically-active drylines much like the ones observed in this study.

7. Eastern Dryline Analysis

A key finding of this study is that many of the drylines that moved atypically far eastward were analyzed incorrectly on the Weather Prediction Center (WPC) / Hydrometeorological Prediction Center (HPC)'s surface analyses (HPC 2013). Hobbs (1996) pointed out that in the case of Rocky Mountain cyclones, the dry troughs are often misanalysed as cold fronts, a mistake than can happen when forecasters use the Norwegian Cyclone Model to describe cyclones in the central United States. Three case studies are shown to illustrate this fact (25 February 2007, 11 February 2009, and 2 April 2010). The surface maps analyzed by the WPF (then HPC) are shown in Figs 7.1, 7.4, and 7.7, HYSPLIT backwards parcel trajectories are shown in Figs 7.2, 7.5, and 7.8, and station plots with 2.78 ^{o}C (5°F) dewpoint contours are overlaid in Figs 7.3, 7.6, and 7.9. The backwards parcel trajectories are taken from three different points around the cyclone, illustrating in all cases the presence of a cP airmass, a cT airmass, and an mT airmass in the typical sectors of a lee cyclone.

The first case, 0300 UTC 25 February 2007 has two cold fronts analyzed in association with the cyclone, one becoming partly occluded (Fig 7.1). Backwards trajectories (Fig 7.2) show the three distinct airmasses, with the airmass over northwestern Louisiana originating over the southwestern United States. The strong dewpoint boundary through Louisiana and eastern Arkansas (Fig 7.3) is therefore the boundary between cT and mT air, and as such is the dryline. The HPC surface analysis for the second case, 1800 UTC 11 February 2009 (Fig 7.4), shows a slightly occluded cyclone over Illinois with an analyzed cold front extending southward through Alabama and a trough extending southwestward through Arkansas and into Texas. Upon closer

examination of the HPC surface map and the station plots (Fig 7.4 and Fig 7.6), it becomes apparent that there is an extremely small temperature gradient along the analyzed cold front and a very large moisture gradient – characteristics associated with a dryline. The trough extending to the southwest has the typical characteristics of a cold front – a large temperature gradient and a smaller moisture gradient. Backwards trajectories from HYSPLIT (Fig 7.5) confirm the origins of the air masses, suggesting that the cold front that is analyzed is actually the dryline, and that the trough that is analyzed is actually the cold front. The surface analysis from 2100 UTC 2 April 2010 (Fig 7.7) shows a surface cyclone located over northern Minnesota with a large cold front draped southward extending through Texas and a second cold front located a little farther west extending from northeastern Nebraska through Colorado. The eastern cold front has a very weak temperature gradient with a much stronger dewpoint gradient, and the western cold front has a much larger temperature gradient. Analysis of the station plots and the air parcel backward trajectories from HYSPLIT (Fig 7.8) reveal that cT air was advected all the way from the Mexican Plateau into southwestern Iowa. This is another case where the cold front analyzed to the east is indeed the dryline, and the cold front analyzed to the west is the actual cold front.

The three cases presented above were not atypical. Many of the drylines identified in this study are not analyzed as drylines in the archived surface analyses. Of the 25 cases that the HPC analyses were available for, only 24% of drylines were analyzed as such. Of the rest of the drylines, 11 were analyzed as cold fronts, 2 were analyzed as stationary fronts, 1 was analyzed as a trough axis, and 5 were not analyzed as any type of boundary. The variation in the analysis of eastern drylines sheds light on the

fact that these boundaries are often times difficult to correctly identify. When drylines move east of the Great Plains, they can often become hybrids between pacific cold fronts and drylines, making them difficult to consistently analyze. Due to the very active upper air patterns that these drylines occur under, air parcels often times can be shown to have been located over the eastern Pacific Ocean just a few days before moving into the eastern portion of the United States. This causes some forecasters to identify these boundaries as pacific cold fronts instead of drylines. However, once the air parcels have moved over the Mexican Plateau, air mass modification takes place, and the air mass (at least the lowest couple of kilometers) takes on the characteristics of a cT airmass with very high temperatures and very low dewpoints. It can be argued that the boundary at the surface between this modified cT airmass and the mT airmass to the east is indeed the dryline instead of a pacific cold front. A three dimensional study would yield more insight into the characteristics of the airmass at higher levels. Another possible explanation for the inconsistencies in the analyses of eastern drylines is that perhaps forecasters are not aware that drylines can and do move farther east than the Great Plains. A hopeful outcome of this study is to increase forecaster awareness of these boundaries in hopes of having drylines analyzed more correctly in the future.

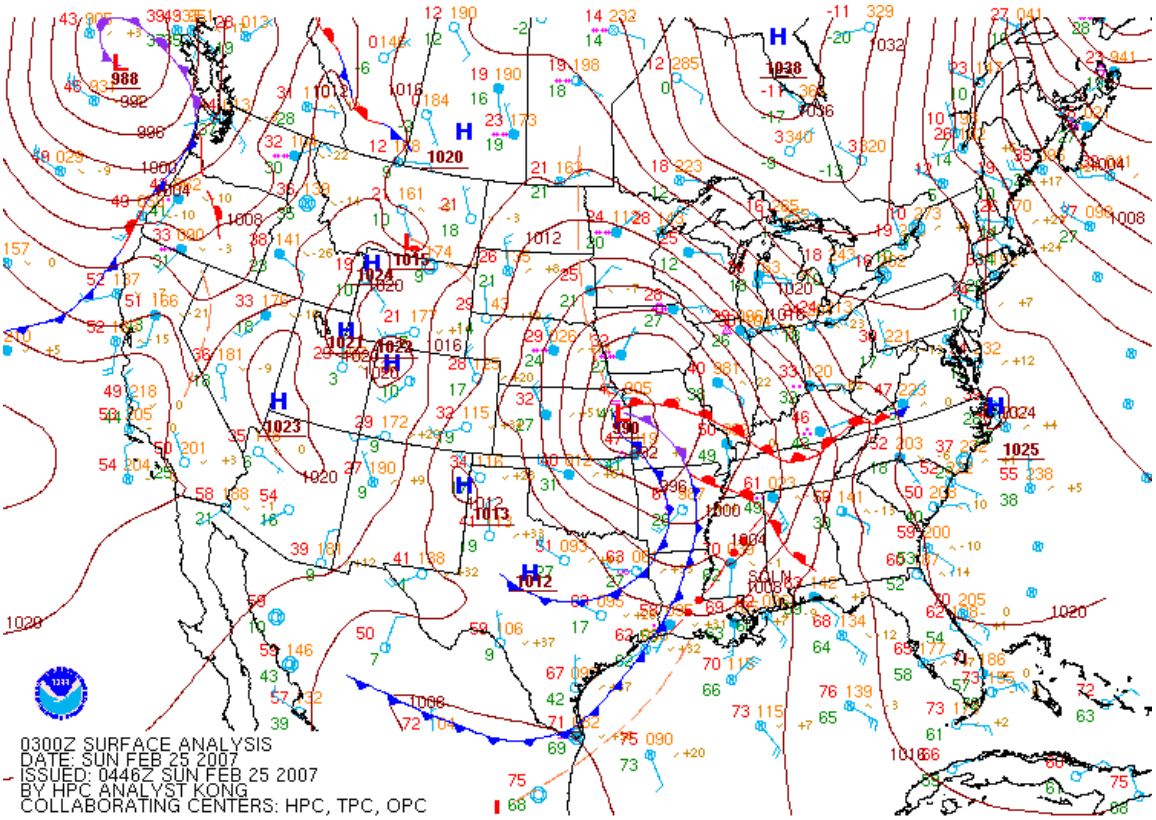

Figure 7.1: Hydrometeorological Prediction Center surface analysis for 0300 UTC 25 February 2007

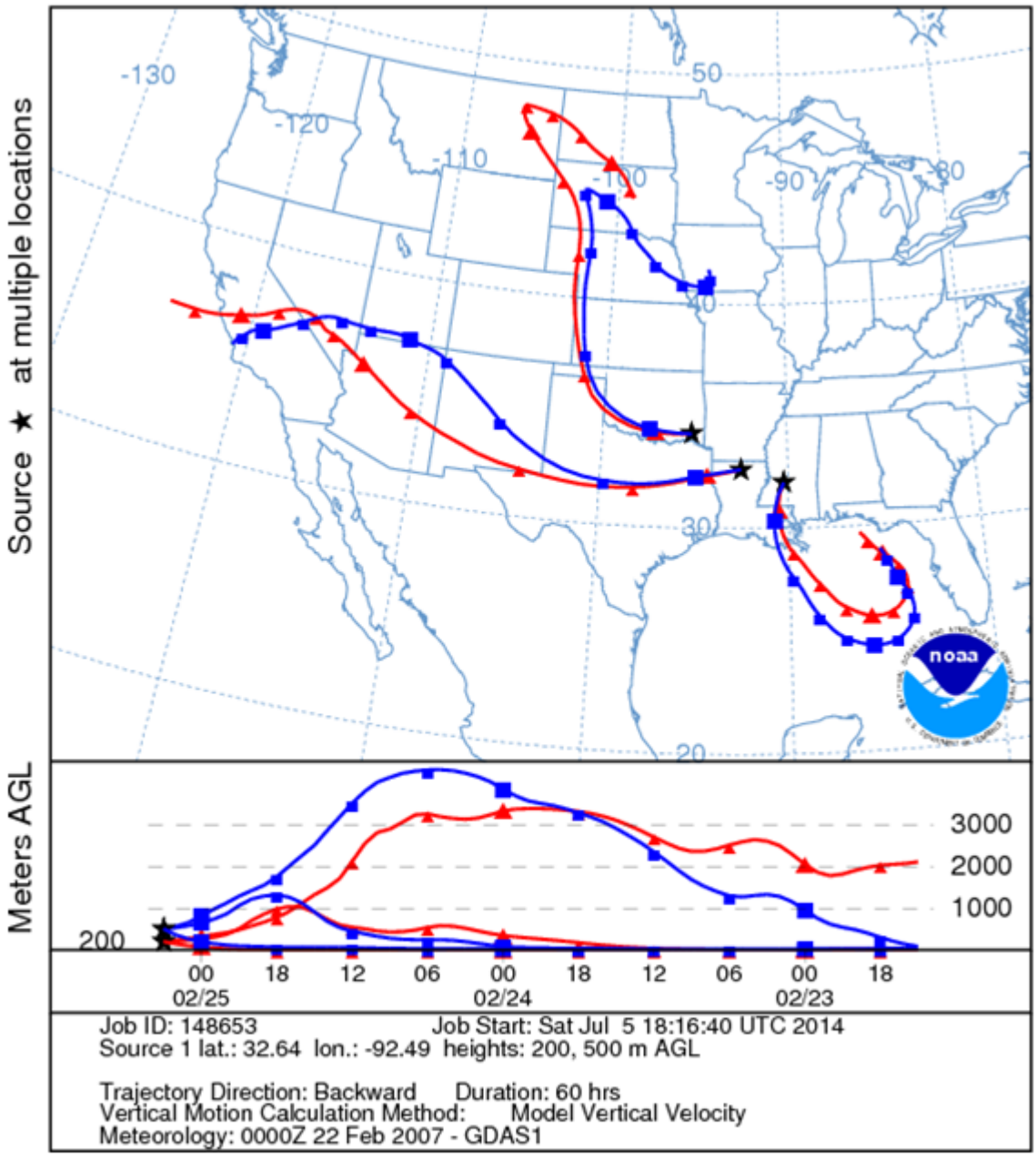

Figure 7.2: 60-hour HYSPLIT backward parcel trajectories for 200 m above ground level (red) and 500 m above ground level (blue) for 0300 UTC 25 February 2007. Smaller markers are plotted every 6 hours, larger markers every 24 hours.

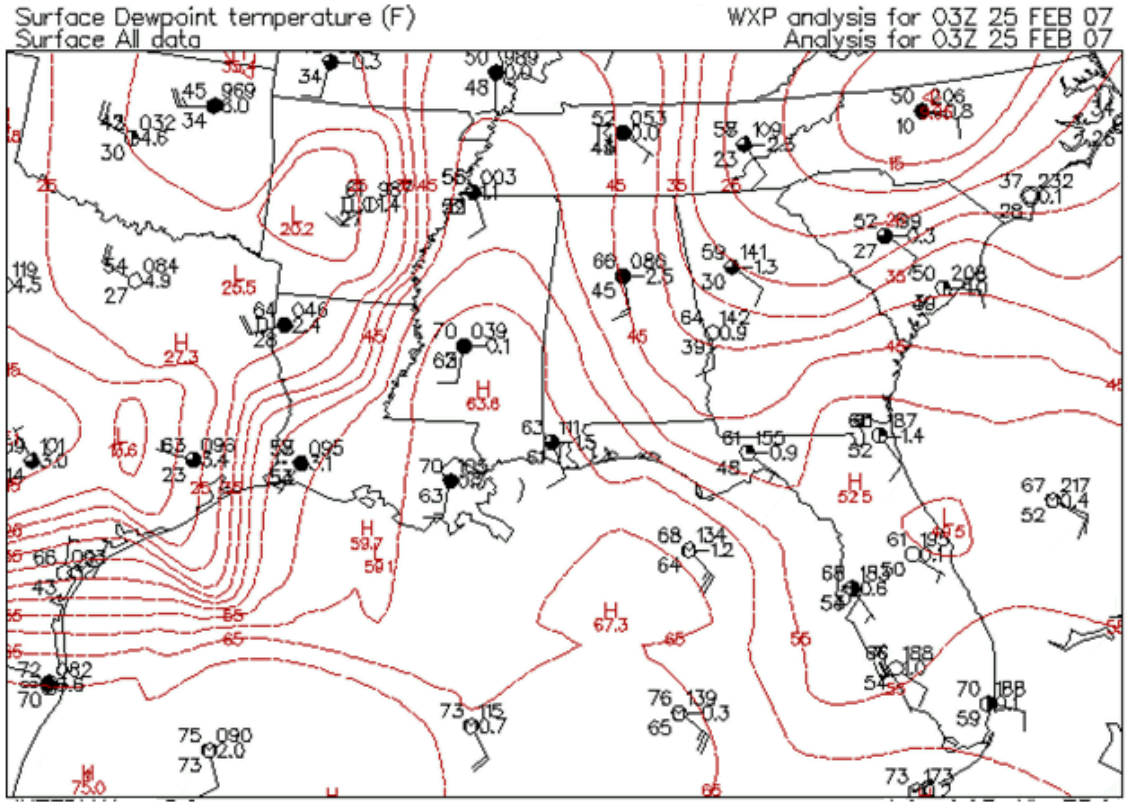

Figure 7.3: Station plots and 5°F dewpoint contours (in red) for 0300 UTC 25 February 2007. Note the strong dewpoint gradient (the dryline) in northern Louisiana/eastern Arkansas. Plot courtesy of the Plymouth State Weather Center [http://vortex.plymouth.edu/].

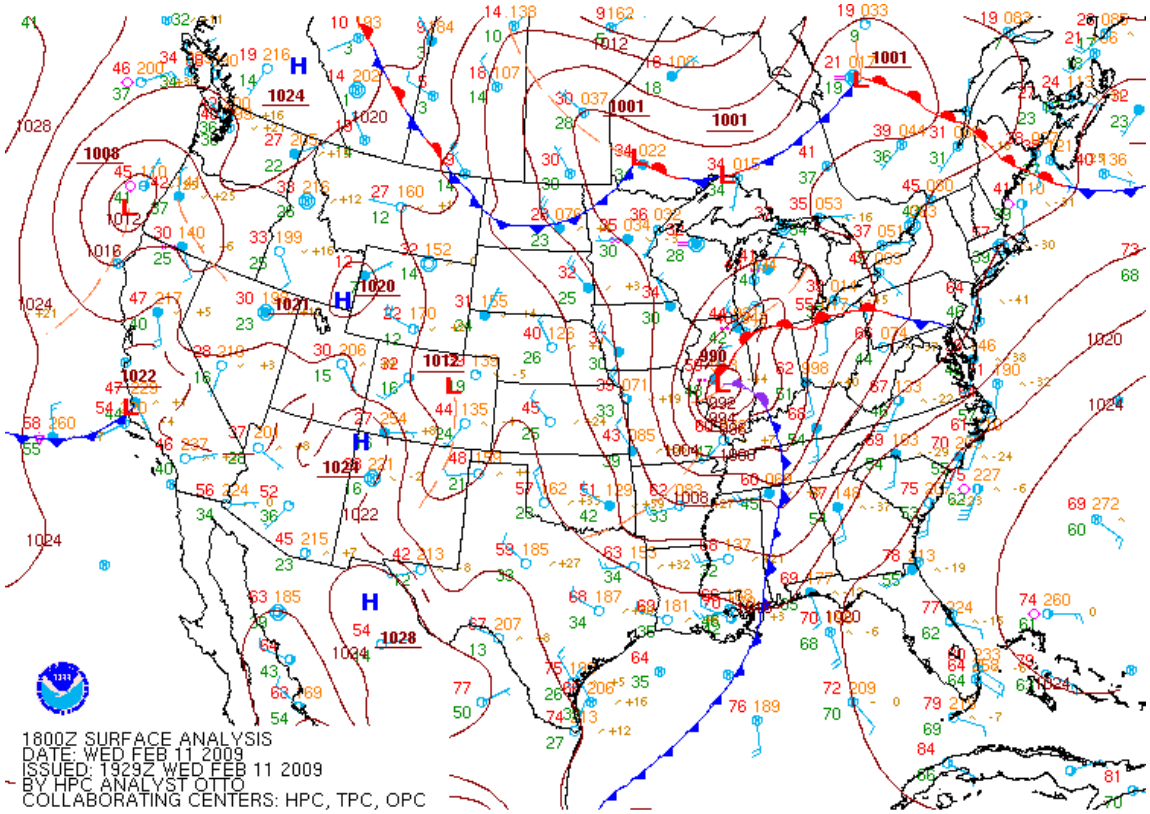

Figure 7.4: Hydrometeorological Prediction Center surface analysis for 1800 UTC 11 February 2009

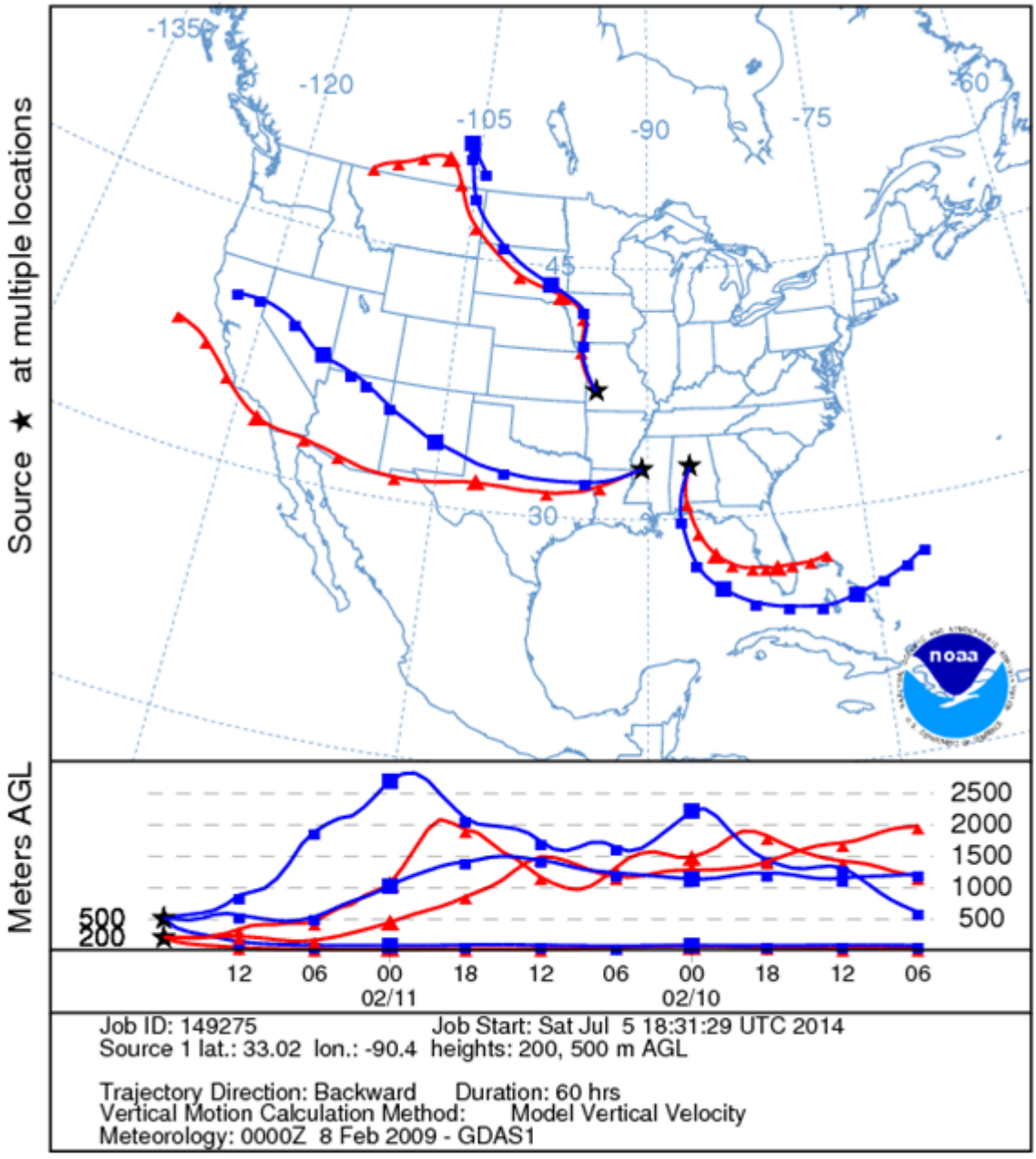

Figure 7.5: 60-hour HYSPLIT backward parcel trajectories for 200 m above ground level (red) and 500 m above ground level (blue) for 1800 UTC 11 February 2009. Smaller markers are plotted every 6 hours, larger markers every 24 hours.

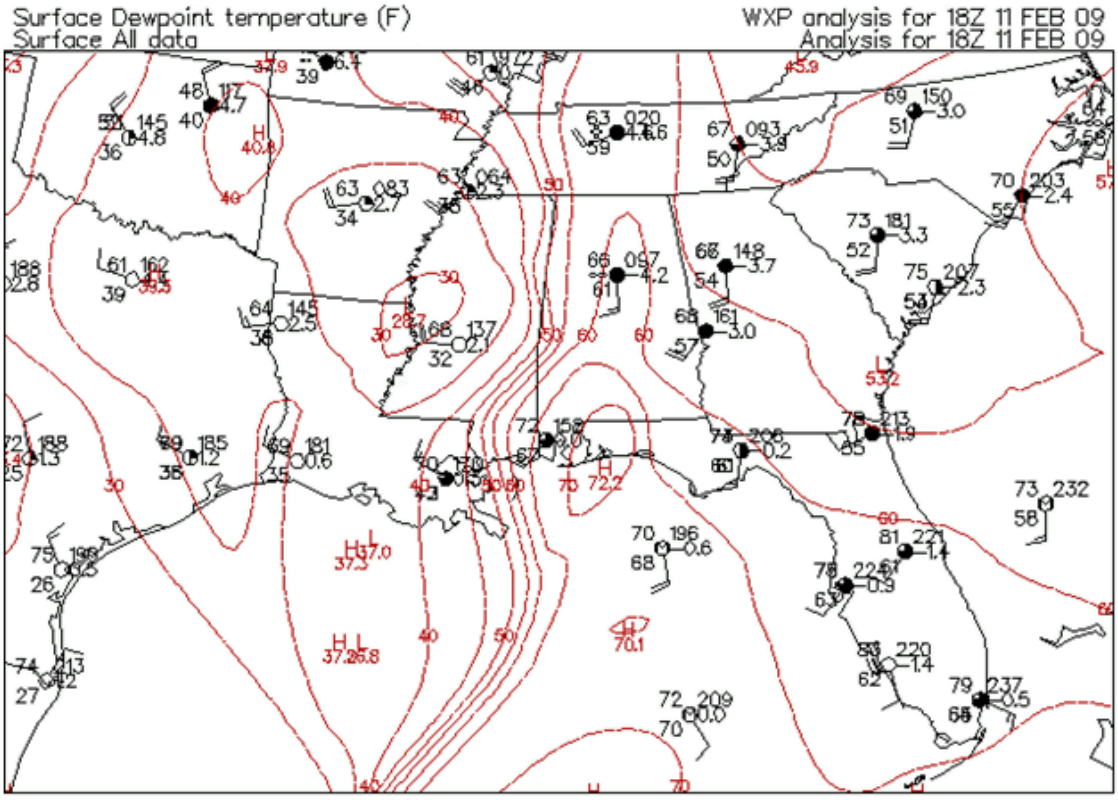

Figure 7.3: Station plots and 5°F dewpoint contours (in red) for 1800 UTC 11 February 2009. Note the strong dewpoint gradient (the dryline) eastern Mississippi. Plot courtesy of the Plymouth State Weather Center [http://vortex.plymouth.edu/].

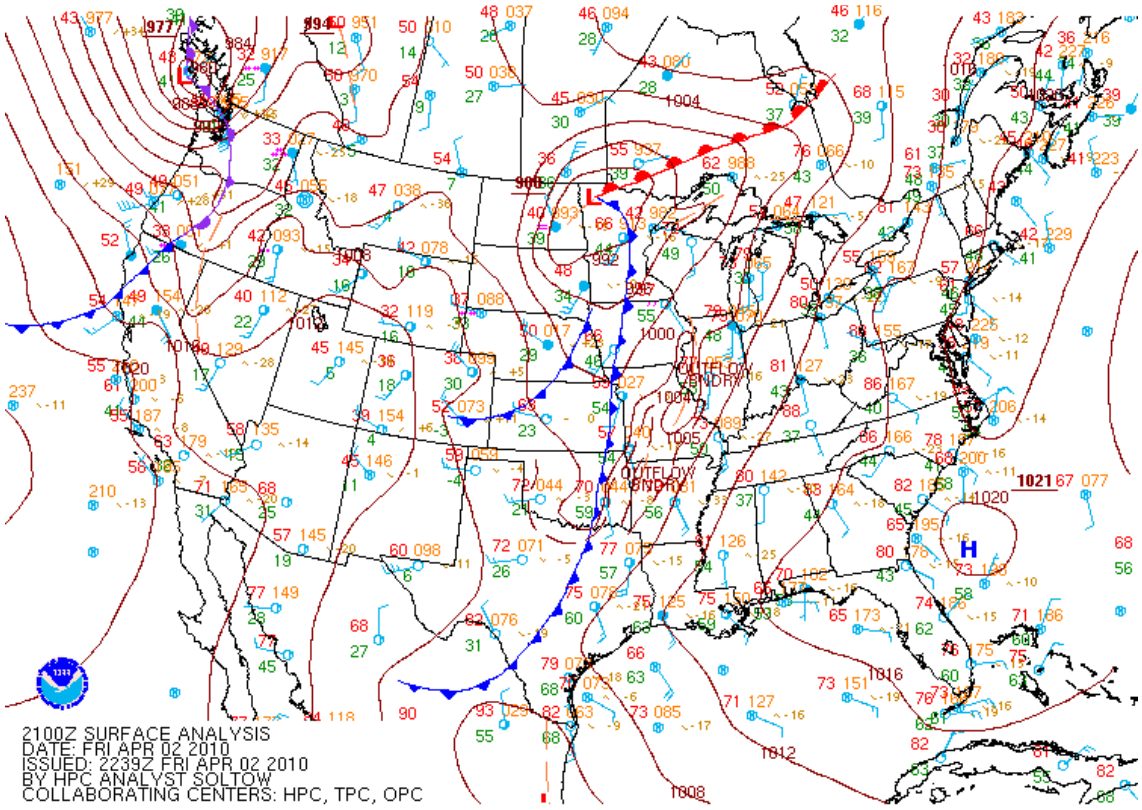

Figure 7.7: Hydrometeorological Prediction Center surface analysis for 2100 UTC 2 April 2010

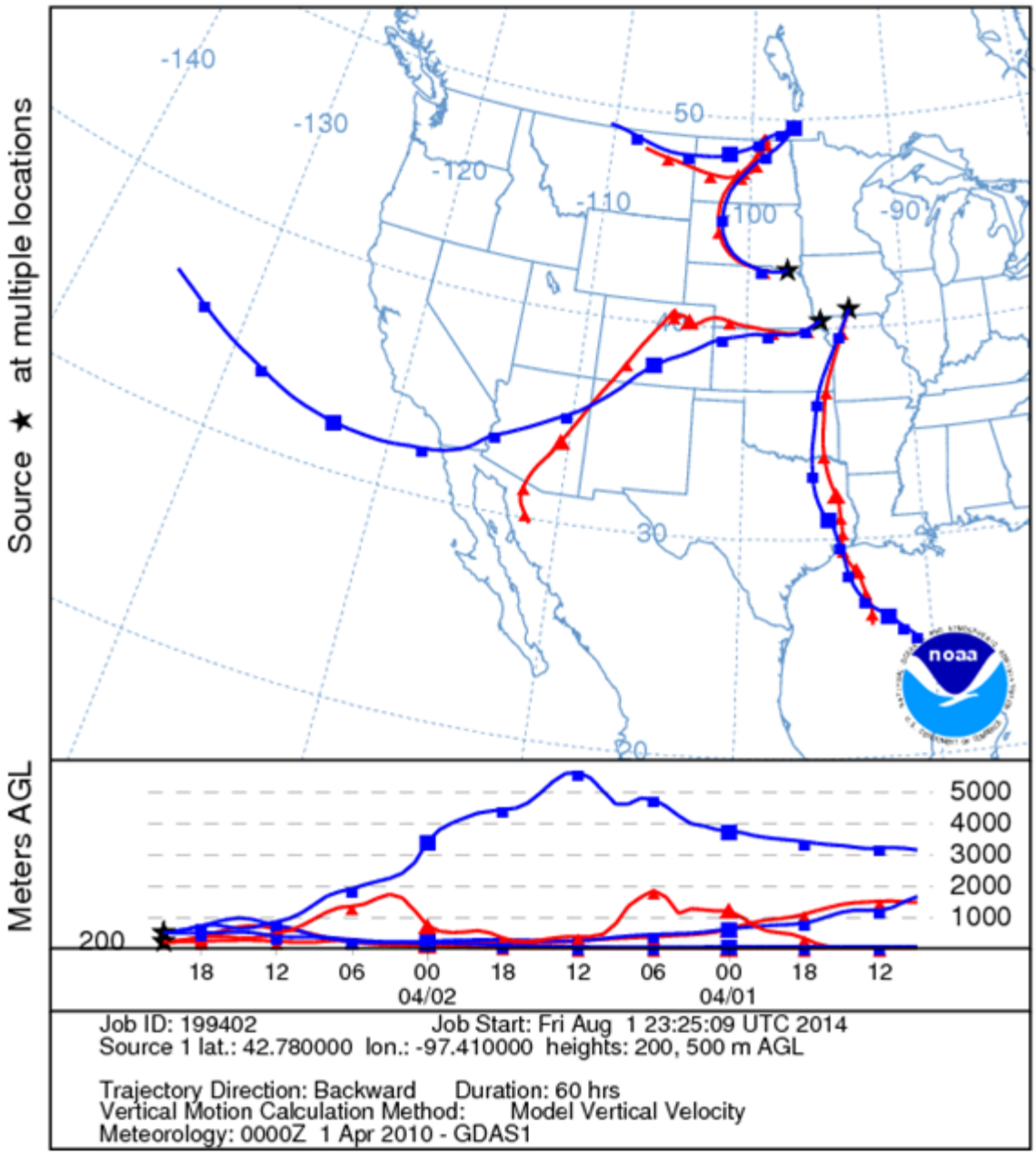

Figure 7.8: 60-hour HYSPLIT backward parcel trajectories for 200 m above ground level (red) and 500 m above ground level (blue) for 2100 UTC 2 April 2010. Smaller markers are plotted every 6 hours, larger markers every 24 hours.

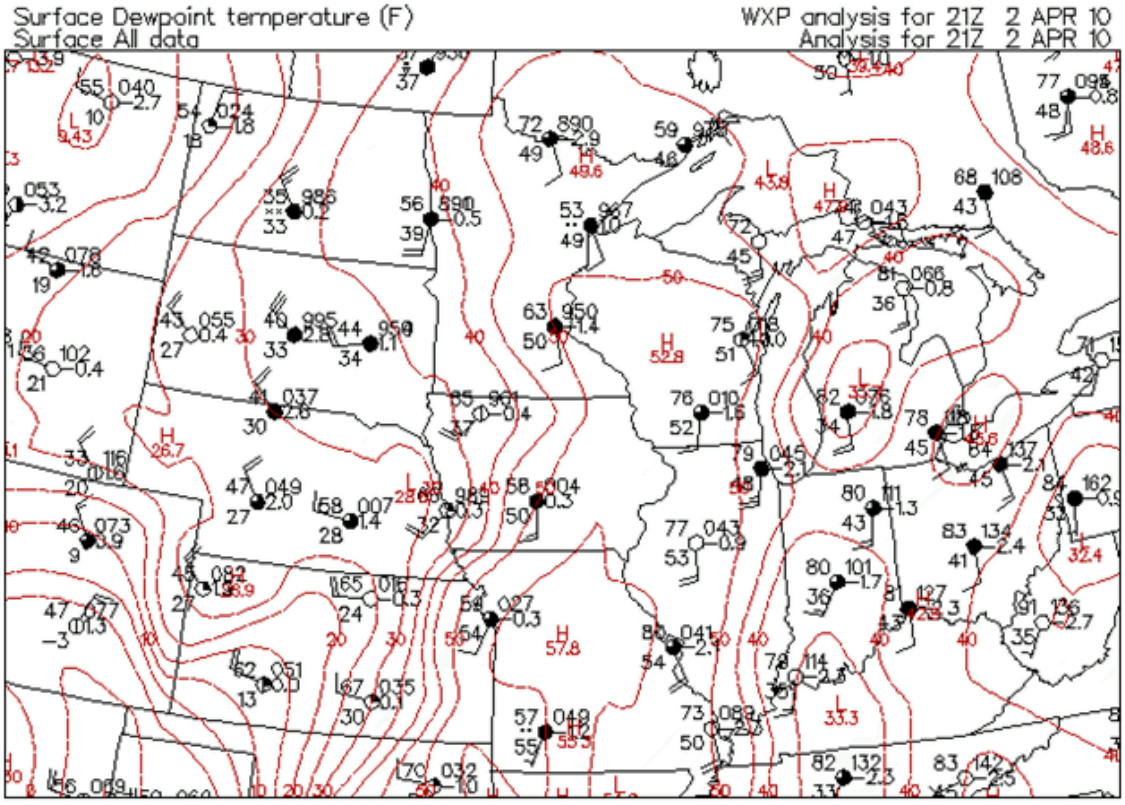

Figure 7.9: Station plots and 5°F dewpoint contours (in red) for 2100 UTC 2 April 2010. Note the strong dewpoint gradient (the dryline) extending through eastern Kansas into southwestern Iowa. Plot courtesy of the Plymouth State Weather Center [http://vortex.plymouth.edu/].

8. Conclusions

A study of eastern drylines was completed in an effort to learn more about these boundaries and to ultimately increase forecaster awareness of drylines east of their typical domain. The primary conclusions for this study are:

- Thirty nine eastern drylines were identified between 1999 and 2013. Arkansas experienced the most dryline passages, followed by Louisiana and then by Missouri.
- The peak in eastern drylines occurred earlier (February through April) than the peak in southern Great Plains drylines.
- A weak correlation between maximum observed dryline longitude and month of the year was observed, with drylines moving farthest east during the winter months. The location of eastern dryline longitude shifted slightly northward throughout the winter and spring.
- Amplified upper-air patterns were observed on the eastern dryline days, with 250 mb jets observed to the west, northwest, or southwest of the drylines. The strongest jets were observed in the Mississippi and Alabama dryline cases. 500 mb geopotential height composites revealed mid-level shortwave troughs generally located to the northwest of the drylines, with slight negative tilts observed in association with the Mississippi River Valley drylines and stronger negative tilts observed in association with the southeastern drylines. Strong mid-level negative height anomalies were seen across the central United States for all days, with mid-level positive height anomalies observed over the northeastern United States. 850 mb analyses showed strong low-level westerlies generally centered to the west of the drylines (again, stronger jets for the

southeastern drylines than for the Mississippi River Valley drylines). 850 mb winds showed a low-level jet east of the dryline and 850 mb temperatures showed strong temperature gradients that likely aided in rapid cyclogenesis at the surface. Sea-level pressure composites showed strong surface cyclones located poleward of the drylines, with the some of the strongest cyclones observed in the southeastern drylines.

- Analysis of the surface maps analyzed by the Hydrometeorological Prediction Center for the dryline days showed that it is not uncommon for eastern drylines to be misanalysed as cold fronts.

Future work will include extending the climatology to a full 30 years, creating additional synoptic composites (e.g. high-amplitude trough events, negatively-tilted trough events, different cyclone strength events), and an in-depth study on the role that eastern drylines play in severe weather outbreaks.

REFERENCES

Atkins, N. T., R. M. Wakimoto, and C. L. Ziegler, 1998: Observations of the finescale structure of a dryline during VORTEX 95. *Mon. Wea. Rev.*, **126,** 525–550.

Barbré, Robert E. Jr., J. R. Mecikalski, K. Knupp, W. Mackenzie Jr., P. Gatlin, and D. Phillips, 2005: An observational analysis of an Alabama dryline event on March 19–20, 2003. *21st Conf. on Wea. Analysis and Forecasting/17th Conf. on Numerical Wea. Prediction*, San Diego, CA, Amer. Meteor. Soc., P1.15. [Available online at https://ams.confex.com/ams/WAFNWP34BC/techprogram/paper_94835.htm.]

Benjamin, S. G., and T. N. Carlson, 1986: Some effects of surface heating and topography on the regional severe storm environment. Part I: Three-dimensional simulations. *Mon. Wea. Rev.*, **114,** 307–329.

Brewer, M. C., C. F. Mass, and B. E. Potter, 2012: The West Coast thermal trough: Climatology and synoptic evolution. *Mon. Wea. Rev.*, **140**, 3820–3843.

Dos Santos Mesquita, M., N. G. KvamstØ, A. Sorteberg, and D. E. Atkinson, 2008: Climatological properties of summertime extra-tropical storm tracks in the Northern Hemisphere. *Tellus A,* **60**, 557-569.

Earth System Research Laboratory, cited 2013: NCEP North American Regional Reanalysis. [Available online at http://www.esrl.noaa.gov/psd/data/gridded/data.narr.html].

Hane, C. E., 2004: Quiescent and synoptically-active drylines: A comparison based upon case studies. *Meteorology and Atmospheric Physics*, **86**, 195-211.

-------, C. E., H. B. Bluestein, T. M. Crawford, M. E. Baldwin, and R. M. Rabin, 1997: Severe thunderstorm development in relation to along-dryline variability: A case study. *Mon. Wea. Rev.*, **125,** 231–251.

-------, C. E., R. M. Rabin, T. M. Crawford, H. B. Bluestein, and M. E. Baldwin, 2002: A case study of severe storm development along a dryline within a synoptically active environment. Part II: Multiple boundaries and convective initiation. *Mon. Wea. Rev*, **130,** 900–920.

Hoch, Joseph, Paul Markowski, 2005: A climatology of springtime dryline position in the U.S. Great Plains region. *J. Climate*, **18**, 2132–2137.

Hoxit, L. R., and C. F. Chappell, 1975: Tornado outbreak of April 3–4, 1974: Synoptic analysis. NOAA Tech. Rep. ERL 338-APCL 37, 48 pp.

HPC, cited 2013: Surface Analysis Archive. [Available online at http://www.wpc.ncep.noaa.gov/archives/web_pages/sfc/sfc_archive.php].

Jones, P. A., and P. R. Bannon, 2002: A mixed-layer model of the diurnal dryline. *J. Atmos. Sci.*, **59,** 2582–2593.

Kalnay, E., and Coauthors, 1996: The NCEP/NCAR 40-Year Reanalysis Project. *Bull. Amer. Meteor. Soc.*, **77**, 437–471.

Knupp, K. R., and Coauthors, 2013: Meteorological overview of the devastating 25 April 2011 tornado outbreak. *Bull. Amer. Meteor. Soc.,* e-view early preprint.

Lin, Yuh-Lang, 2010: *Mesoscale dynamics*. Cambridge University Press, 646 pp.

Locatelli, J. D., M. T. Stoelinga, and P. V. Hobbs, 2002: A new look at the Super Outbreak of tornadoes on 3–4 April 1974. *Mon. Wea. Rev.*, **130**, 1633–1651.

Maddox, R. A., M. S. Gilmore, C. A. Doswell III, R. H. Johns, C. A. Crisp, D. W. Burgess, J. A. Hart, and S. F. Piltz, 2013: Meteorological analyses of the Tri-State tornado event of March 1925. *Electronic J. Severe Storms Meteor.,* **8** (1), 1–27.

Mesinger, Fedor, and Coauthors, 2006: North American Regional Reanalysis. *Bull. Amer. Meteor. Soc.*, **87**, 343–360.

Moller, A. R., 2001: Severe local storms forecasting. *Severe Convective Storms, Meteor. Monogr.,* No. 50, Amer. Meteor. Soc., 433–480.

Peckham, S. E., and L. J. Wicker, 2000: The influence of topography and lower-tropospheric winds on dryline morphology. *Mon. Wea. Rev*, **128,** 2165–2189.

Rasmussen, E. N., J. M. Straka, R.t Davies-Jones, C. A. Doswell, F. H. Carr, M. D. Eilts, and D. R. MacGorman, 1994: Verification of the Origins of Rotation in Tornadoes Experiment: VORTEX. *Bull. Amer. Meteor. Soc.*, **75**, 995–1006.

Rhea, J. O., 1966: A study of thunderstorm formation along dry lines. *J. Appl. Meteor.*, **5,** 58–63.

Robinson, P. J., 1998: Monthly variation of dew point temperature in the coterminous United States. *International Journal of Climatology*, **18**, 1539-1556.

Schaefer, J. T., 1974: The lifecycle of the dryline. *J. Appl. Meteor.*, **13,** 444–449.

----------, J. T., 1986: The dryline. *Mesoscale Meteorology and Forecasting,* P. S. Ray, Ed., Amer. Meteor. Soc., 549–572.

Schultz, D. M., C. C. Weiss, and P. M. Hoffman, 2007: The synoptic regulation of dryline intensity. *Mon. Wea. Rev.*, **135,** 1699–1709.

Shafer, J. C., and W. J. Steenburgh, 2008: Climatology of strong intermountain cold fronts. *Mon. Wea. Rev.*, **136**, 784–807

Sun, W. Y., and C. C. Wu, 1992: Formation and diurnal variation of the dryline. *J. Atmos. Sci*, **49,** 1606–1619.

Weckwerth, T. M., and Coauthors, 2004: An overview of the International H_2O Project (IHOP_2002) and some preliminary highlights. *Bull. Amer. Meteor. Soc*, **85,** 253–277.

--------, C. C., H. B. Bluestein, and A. L. Pazmany, 2006: Finescale radar observations of the 22 May 2002 dryline during the International H2O Project (IHOP). *Mon. Wea. Rev.*, **134**, 273–293.

Wilks, D. S., 2011: *Statistical methods in the atmospheric sciences: 3rd edition*. Elsevier Science, 704 pp.

Ziegler, C. L., and E. N. Rasmussen, 1998: The initiation of moist convection at the dryline: Forecasting issues from a case study perspective. *Wea. Forecasting*, **13,** 1106–1131.

---------, C. L., W. J. Martin, R. A. Pielke, and R. L. Walko, 1995: A modeling study of the dryline. *J. Atmos. Sci.*, **52,** 263–285.